

An Air and Water Stable Semiconducting Polymer: Polyfluorene TetraPhenyl Diamine



Francesco Maddalena

Nanoscience - MSC^{Plus}

Physics of Organic Semiconductors

Rijksuniversiteits Groningen



Index

	Page
Abstract	2
1- Introduction	3
1.1 – Semiconducting polymers and organic materials	3
1.1.1 – The basic structure of semiconducting polymers	3
1.1.2 – Conduction and Hopping transport	5
1.1.3 – Polarons	7
1.1.4 – Multiple trapping and release model	8
1.1.5 – Charge injection	9
1.2 – The field-effect transistor	10
1.2.1 – Basic working of the FET	10
1.2.2 – The field-effect mobility	12
1.2.3 – The effect of oxygen and water on the organic FET operation	14
1.3 – Light-emitting diodes and hole-only devices	16
1.4 – Aim of this research	18
2 – Materials and methods	19
2.1 – Chemicals and materials	19
2.2 – Sample preparation	19
2.2.1 – Preparation of polymer solutions	18
2.2.2 – Preparation of thin-film transistors	20
2.2.3 – Preparation of LED and HOD	20
2.3 – Measurements	21
2.3.1 – FET measurements	21
2.3.1 – LED and HOD measurements	21
2.3.1 – Thickness measurements	21
3 – Results	22
3.1 - P3HT and PFTPDA in vacuum	22
3.2 - P3HT and PFTPDA under the influence of air	24
3.3 - P3HT and PFTPDA under the influence of water	28
3.4 - PFTPDA Light-emitting diodes	30
3.5 – Mobility data from the measurements	31
4 – Conclusions and discussion	33
5 – References	35

Abstract

The stability of semiconducting polymers in presence of oxygen and water has always been a problem in the development of organic semiconductor technology and certain types of devices require coming in contact with air and water. It is thus important to find air stable and water stable semiconducting polymer materials, which will have prolonged lifetime compared to non air or water stable materials in devices like light-emitting diodes (LED) and field-effect transistors (FET). Air and water stable semiconducting polymers will open doors for new types of devices like biosensors. The stability must not simply be chemical (resistance to degradation) but the working of a device with an organic semiconductor must also be stable (resist the influence of doping). In this research we compare a novel material, PFTPDA, which is supposed to be air and water stable, with RR-P3HT a widely studied material which is chemically air stable, but is also quickly doped by molecular oxygen. The results of measurements in FET under vacuum and in presence of air or water showed that PFTPDA is more air stable than RR-P3HT and is doped by oxygen in a much slower process. PFTPDA has also some water stability and, although its mobility decreases, it still retains its characteristics after been in contact with water for one hour. Unfortunately the mobility of the material is still low, and light emission in LED is also poor. The stability in air of PFTPDA and its partial stability in water can be explained by the energetic position of its HOMO level, which is deeper than the HOMO of RR-P3HT, hence PFTPDA has a higher redox potential making it more difficult to oxidize by oxygen and water. The results also suggest that the polymer might contain traps and the conduction of charges in it is trap limited.

1. - Introduction

1.1– Semiconducting polymers and organic materials

Polymers (and organic materials in general) are strong, light-weighted, relatively easy to process, recyclable and adaptable. Since the discoveries of the first polymers, these materials have been strong competitors in many economic and technological fields. Yet for a long time these material have been reputed only to be insulators, but since the discovery of polyacetylene and its conducting properties¹ in 1977, organic materials are becoming more and more prominent as semiconductors and conductors (usually when these materials are doped) for a variety range of (novel) applications in electronics and opto-electronics, such as logics, sensors, organic light-emitting diodes and solar cells. In the last few years conducting and semiconducting polymers have also aroused interest in biosensor and bioelectronics technology.

1.1.1– The basic structure of semiconducting polymers

Semiconducting polymers have a basic difference from inorganic semiconductors: their molecular nature. The carbon atoms that constitute the backbone of the polymer can form basically two types of bonds with each other: a σ -bond and a π -bond. Carbon atoms have 6 electrons and the following electronic configuration: the 1s orbital is filled and so is the 2s. The remaining 2 electrons are placed in the 2p orbitals ($2p_x$, $2p_y$ and $2p_z$) and divided according to Hund's Rule, hence the $2p_x$ and $2p_y$ orbitals will have one electron leaving $2p_z$ empty. According to LCAO-MO theory linear combinations of the atomic orbitals (LCAO) give rise to the molecular orbitals (MO). While the 1s orbital does not contribute at all the 2s and 2p orbitals can hybridize in three possible configurations: sp^3 , sp^2 and sp . In the sp^3 hybridization the 2s orbital is hybridized with all three 2p orbital giving rise to four sp^3 -orbitals that point at the vertex of a tetrahedron (Figure 1.a) like in the methane molecule. In the sp^2 hybridization the 2s orbital is hybridized with two 2p orbitals giving rise to three sp^2 orbitals and one 2p orbital is left (Figure 1.b). For the sp hybridization the 2s orbital hybridizes only with one 2p orbital leaving two 2p-orbitals unchanged.

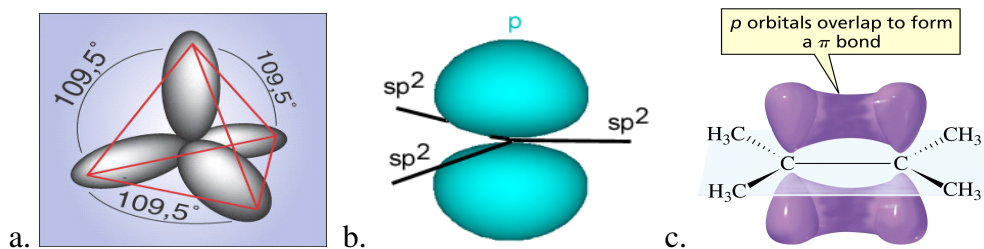


Fig.1 – Orbitals in the sp^3 -hybridization (a.) and the sp^2 -hybridization (b.) and a molecule with a π -bond (c.).

According to LCAO-MO theory the hybridized atomic orbitals will combine to form molecular orbitals. Carbon can form two types of bonds: σ -bonds, which are the result of the interaction of sp^3 (or sp^2 or sp) orbitals with the orbitals of another atom (like 1s of Hydrogen in methane) and π -bonds, which are the result of the interaction of the p-orbitals of the two carbons. Carbon with sp^2 hybridization will form 1 π -bond (see fig.

1c.) and carbon with sp hybridization state will form two². The π -bonds are essential for the conduction in polymers.

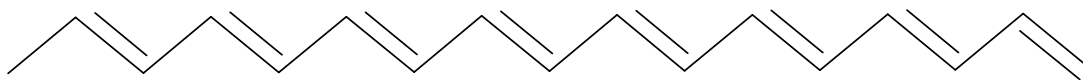


Fig. 2- A conjugated carbon backbone

The key feature of a conducting or semiconducting polymer is the presence of a conjugated system in their molecular structure, which is an extended π -bond system along the backbone of the polymer molecule (Figure 2). In a conjugated molecule the electrons in the π -bond can be excited while the electrons in the σ -bonds in the backbone maintain the structural integrity of the molecule, hence a conjugated polymer can be electronically excited without being destroyed. Moreover an electron (or hole) in a conjugated system will be delocalized within the conjugated segment.

The HOMO (highest occupied molecular orbital) and the LUMO (lowest unoccupied molecular orbital) determine the energy gap of the semiconducting polymer. In a conjugated molecule the HOMO and the LUMO are given by the highest occupied (bonding) π -orbital and the lowest unoccupied (anti-bonding) π -orbital, respectively. The number of π -levels present in a conjugated molecule equals the number of original p-orbitals, hence the longer the conjugated chain the more π -levels will be present.

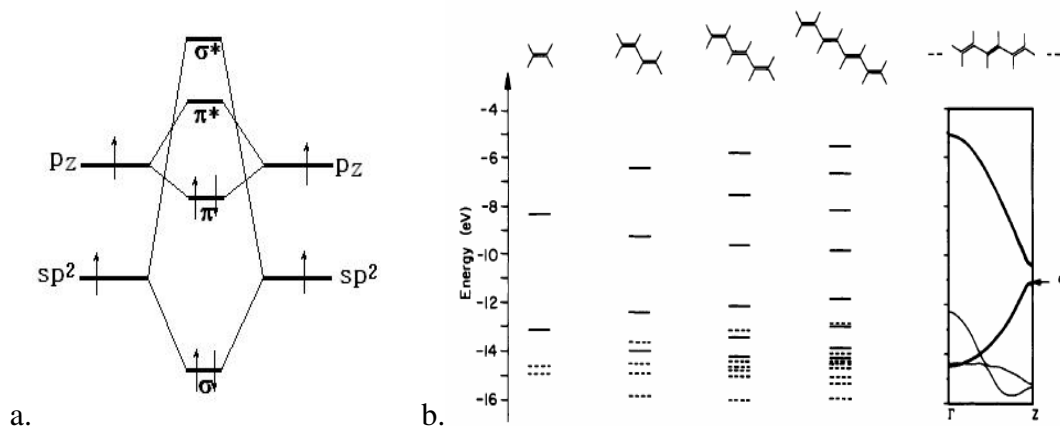


Fig. 3 - (a.) Electronic scheme of ethylene involving only the electrons in the σ -bond and π -bond. (b.) Relationship of the energy levels around the Fermi level and the chain length showing the band structure build up of the polymer (Hoffmann et. al. 1991)

The spacing between the different levels and the gap between HOMO and LUMO will diminish as the number of levels increases. For a long conjugated chain the levels will be so close that they will give rise to energy bands similarly to the ones present in inorganic semiconductors. The energy difference between the HOMO and the LUMO though will not disappear³, giving rise to a band gap as Figure 3 shows.

Semiconducting polymers are characterized by a conjugated system but their structure, determined by the monomers and type of polymerization is various. Different types of side chains, region-regularity and presence of hetero atoms in the backbone itself (such as sulphur, oxygen or nitrogen, which can contribute with their p-orbitals to the conjugation)

contribute to change the physical properties of the polymer such as solubility and to tune its electronic structures. Some polymers, however, present an exception, such as polyaniline, which can show a high mobilities when doped, but it does not present a conjugated system.

1.1.2- Conduction and Hopping transport

The conduction mechanism through conjugated polymers is very different than the one in inorganic semiconductors, which is dependent on band transport^{4, 5}. Conjugated polymers do present a band structure due to their conjugated nature, yet they lack intrinsic mobile charges, like the electrons and holes present in e.g. silicon. In polymers mobile charges must be created by exciting the electrons from the HOMO to the LUMO, e.g., by photons, or by injection charges from the electrodes or by chemical dopants. Unlike inorganic semiconductors conjugated polymers do not have an extended band structure. Solid-state polymer materials are very disordered, especially if cast from solution and still contain traces of solvents and impurities. Some polymers, showing regioregularity, can form polycrystalline structures. Furthermore, the forces that bound the polymer chains together are Van Der Waals forces which are much weaker than the strong forces that bound inorganic semiconductors, so conjugated polymers have relatively narrow energy bands (the HOMO and the LUMO) that can be easily disrupted by disorder⁶.

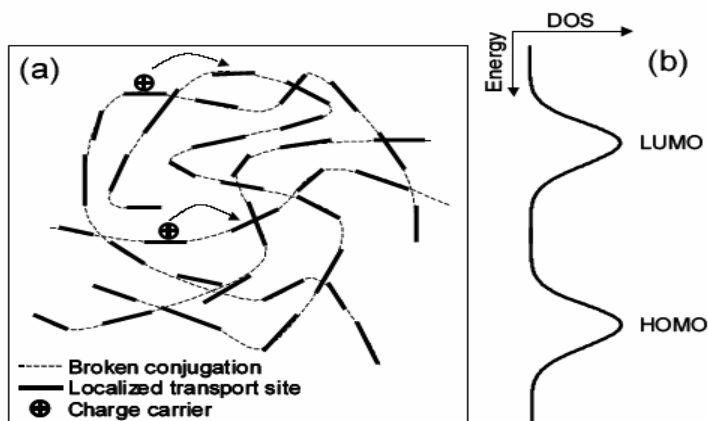


Fig. 4: (a) Schematic view of polymer chains broken up in conjugated segments, which are represented as charge transport sites, between which the charge carriers hop. (b) A representation is given of the smeared out density of states, which is often approximated by a Gaussian distribution for the HOMO and LUMO levels (E. Meijer- PhD. Thesis - Charge Transport in Disordered Organic Field-Effect transistors-fig. 1.4)

The mobile charges in polymers are delocalized in the energy bands formed by the extended π -conjugated system, yet the segments of perfectly conjugated chains are usually not very long and are typically limited to lengths of 5 nm and are separated by defects such as chemical defects (e.g., breaking of a double bond) and structural defects (e.g., kinks in the chain, chain termination or co-planarity broken by chain twists). Defects also create traps for the charges, hence the mobile charges are fairly localized.

The consequences of the disorder and the defects is that it is not possible anymore to consider the conjugate polymer as having two energy bands separated by a gap like in

inorganic semiconductors. Instead we must treat the density of states (DOS) of the energy bands as a Gaussian distribution function⁷ as shown in Figure 4.b which is also confirmed by spectroscopic measurements. The shape and characteristics of the Gaussian DOS strongly depends on the disorder and the properties of the polymer and are usually difficult to determine experimentally.

The localization of mobile charges due to structural disorder in conjugated polymers described above clearly states that band transport as we know it for metals and inorganic semiconductors does not occur in semiconducting polymers. Conduction through conjugated polymers is typically described by hopping transport, which is a phonon assisted tunneling mechanism from site to site. Hopping can be schematically summarized by describing the movement of the localized charge carriers (electrons or holes) along the material as a series of tunneling jumps from site to site. The sites in the case of polymers are the conjugated parts of the chains or eventual traps. Hopping transport occurs around the Fermi level. The Fermi level is defined as the highest occupied energy level at a temperature of 0 K and its position is determined by the charge neutrality condition of the system. At temperatures higher than zero the distribution of occupied levels around the Fermi level is described by the Fermi-Dirac distribution, such that some levels above the Fermi level are occupied and others below the Fermi level are empty⁸.

There are many different theoretical models for hopping transport, but most of them are based on the single phonon jump rate description⁹ where the hopping rate v_{ij} between an occupied site i and an adjacent unoccupied site j , which are separated in energy by $E_i - E_j$ and in distance by R_{ij} , is described by:

$$v_{ij} = v_0 \exp(-2\gamma R_{ij}) \exp\left(-\frac{E_i - E_j}{k_B T}\right) \quad \text{for } E_i > E_j \quad (1.a)$$

and:

$$v_{ij} = v_0 \exp(-2\gamma R_{ij}) \quad \text{for } E_j > E_i \quad (1.b)$$

where γ^{-1} quantifies the wavefunction overlap between the sites and depends on the molecular shape, size and stacking of the polymer chains, v_0 is a pre-factor, and k_B is Boltzmann's constant. The first exponential term in equation **1.a**, corresponding to equation **1.b**, describes the tunneling rate of the electrons, while the second exponential term of equation **1.a** describes the emission or absorption of a phonon that aids the hopping. Because the Hopping process is not only field-assisted but also phonon-assisted (in contrast with band transport), hence it is also thermally activated. The electrons can either favor to hop over a longer distance with low energy difference between the sites than over a shorter distance with higher energy difference. This is depends on the structural and energetic disorder of the material. Figure 5 gives a graphical representation of band and hopping transport.

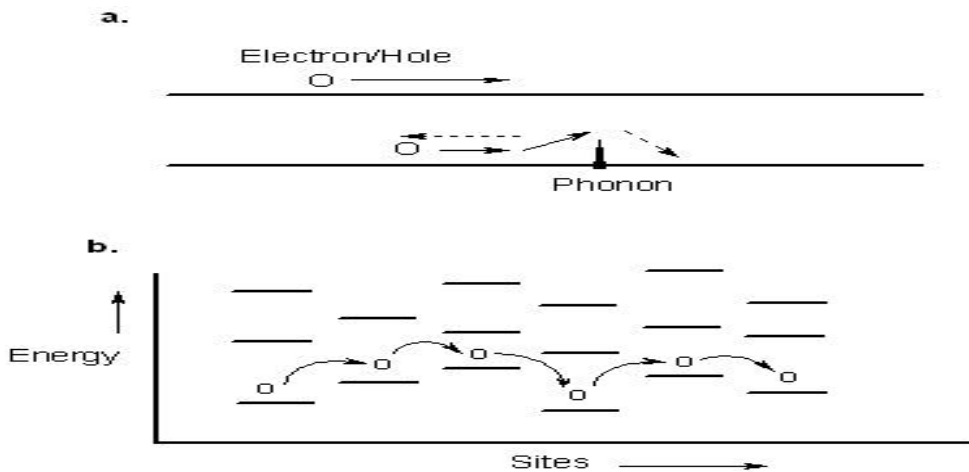


Fig. 5: Charge transport in solids. (a.) Band transport. The band of a perfect crystal is described as a straight line where the delocalized free carrier moves. No matter how perfect the crystal is, the symmetry is always disrupted by phonons (lattice vibrations) that scatter the charge carriers. Since lower temperatures mean less lattice vibrations, the mobility of the charge carriers decreases with increasing temperature. (b.) Hopping transport. In this type of transport the carrier is localized due to disorder, defects or self-localization (e.g. polarons) and hops from site to site with the essential help of lattice vibrations. The mobility of the carriers for this type of transport increases with the increase of temperature.

1.1.3– Polarons

Organic materials present a strong electron-phonon coupling. An effect of such interaction is the apparent increase in mass of the electron (or hole) because the charge drags the heavy ion cores along with it when they move. This effect is very strong in ionic material such as salts and weaker in molecular materials. In an insulator or in an organic semiconductor such interactions between the electron or hole and its strain field (phonon cloud) form a quasiparticle called *polaron*^{8, 10}. A schematic view of a positive polaron in a polymer is given in Figure 6.a. In the chemical terminology polarons are charged radicals, either a radical cation (positive polaron) or a radical anion (negative polaron). Together with the structural disorder mentioned above, polarons are also a cause for the localization of charge in polymer and organic semiconductors.

In organic materials the formation of polarons originates from an excess charge carrier on a conjugated polymer chain that can minimize its energy by a local lattice deformation. Chemically speaking this is nothing else than the formation of radical cations or anions. This happens when first a radical is formed, for example by the separation of the two electrons that form a π -bond. Then two radicals are formed (a soliton pair). If one of the two radical electrons is removed then a radical electron and a positive charge will be left, giving rise to a positive polaron. If one electron is added to one of the radical electrons then the electrons will form an electron pair, negatively charged. This negative charge together with the radical electron left will give rise to a negative polaron.

We can see in Figure 6.a. that where the radical action (or positive polaron) is localized the conjugation of the polythiophene polymer (shift in the position of the double bonds) is different than outside the region where the polaron is localized. This shift in the position of the double bonds is the cause of the lattice distortion in the structure of the polymer¹¹.

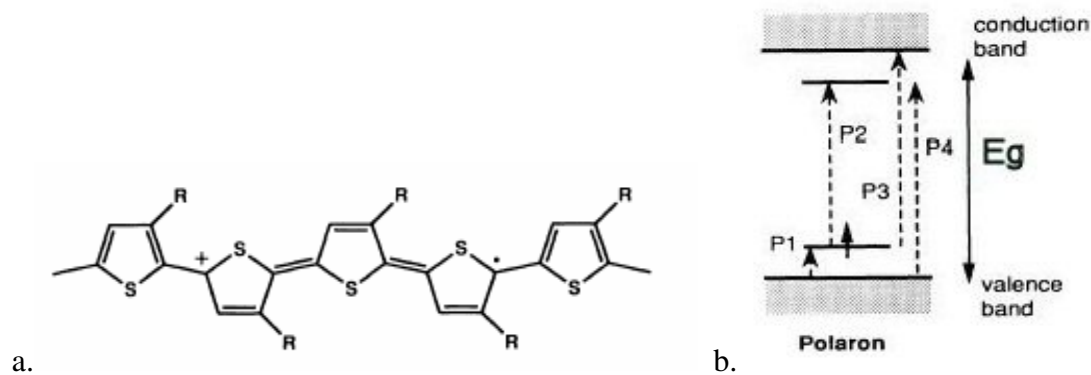


Fig. 6: (a). Schematic diagram of a positively charged polaron on a polythiophene chain. From a chemical point of view this represents a radical cation. (b.) Energy-level scheme and optical transitions for a positively charged polaron. Different optical transitions are shown in the figure: P1: transition from the valence band to the first polaron level, P2: transition from the first to the second polaron level, P3: transition from the first polaron level to the conduction band, P4: transition from the valence band to the second polaron level (Adapted from: Ziemelis et. al. *Phys. Rev. Lett.* **66** p.2231, 1991)

Since these quasiparticles cause a distortion of the lattice of the material caused by the charge, the energy levels of the polarons must split off the HOMO (valence band) and the LUMO (conduction band) and reside in the energy gap of the semiconductor as it is shown in Figure 6.b. These energy levels are not simply theoretical but have often been observed in spectroscopic measurements on conjugated polymers. If a conjugated polymer is highly doped the large number of polaron levels arisen may form a band structure, in that case we speak of *polaron bands*. These bands give rise to metallic conduction to (highly) doped polymers.

1.1.4– Multiple trapping and release model¹²⁻¹⁵

Although the general structure of polymer films is amorphous, some polymers, like regioregular poly(3-alkylthiophene)s, present a polycrystalline structure. Organic molecules and oligomers also often present this type of structure. These crystalline structures are called ‘grains’ or crystallites and are separated from each other by amorphous grain boundaries.

In the case of polycrystalline materials the theory of charge transport explained above must be modified. Inside the grains the charge carriers can move in the delocalized bands formed by the crystalline structure, yet these bands cease to exist at the grain boundary, where the mobile charges remain trapped (in other words: localized) in states that are called ‘traps’. These traps are caused by the disorder around the grains, where the conjugation of the chains is often broken and by impurities present in the film. The limiting factor in the charge transport in these polycrystalline polymers is the release of trapped charges which is much slower than band transport inside the grains and shows many similarities to hopping transport with the substantial difference that the D.O.S. of the traps is of an exponential form and not Gaussian like in hopping transport described above. This process is also thermally activated. In this type of transport the charges that are first transported within the grains in the band structure often get trapped in localized states when they reach the grain boundary. Then the charges have to get released from these states in a way similar to hopping.

1.1.5–Charge injection^{4, 16, 17}

Charge conduction through the bulk of the organic semiconductor is not the only important issue in charge transport in devices. The injection of charges from the (metal) electrodes into the organic semiconductor is also critical and can represent a limitation on transport if the injection barrier at the contacts is high. To understand the injection of charges into a material from another it is important to know what happens when two materials come into contact, more explicitly when a metal and a semiconductor make contact.

When a metal and a semiconductor come into contact the Fermi levels (which can also define as the chemical potential of the electrons in a material) align to achieve equilibrium. The alignment occurs by transfer of electrons from the material with the higher Fermi level to the one with the lower Fermi level causing an accumulation of charges that gives rise to a potential difference. The material that had the lower Fermi level will be negative and the material with the higher Fermi level will be positively charged. The potential build up then shifts the levels of the semiconductor, giving rise to ‘band bending’ nearby the contact with the metal. Also due to the low conductivity and low carrier density of the semiconductor a carrier gradient over large distances may arise (several nanometers), where at the contact the concentration of the carriers is the lowest. This region is called the *depletion region*. When the number of carriers is extremely low compared to the normal carrier concentration the region is called ‘fully depleted’ and greatly hinder charge transport.

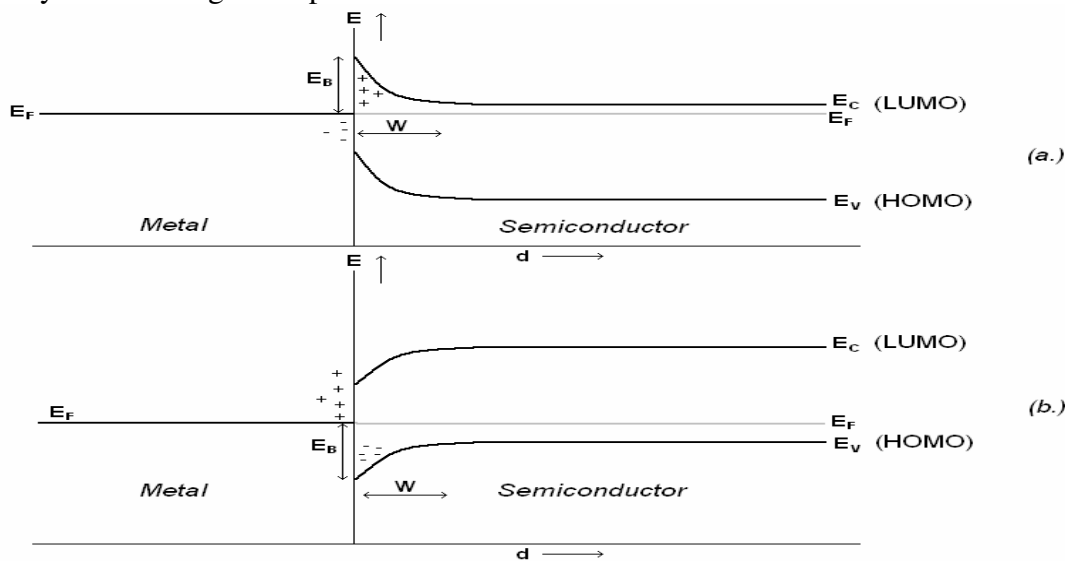


Fig. 7: Schottky barrier for electrons (a.) and holes (b.) to be injected from the metal to the semiconductor. The contact between a metal electrode and a semiconductor is shown after alignment of the Fermi energy E_F and band bending, at thermal equilibrium in a graph of energy (E) against the distance d around the contact. Here E_C and E_V are the energies of the conduction and the valence band respectively. For organic materials these correspond to the LUMO and HOMO respectively. W is the width of the depletion region.

In a device, such as a LED or a FET one must start from the equilibrium situation established after contact, especially it is important to see in the injection of a charge carrier is favored or hindered. If the Fermi level of a metal is *higher* than the valence band (HOMO level in organic materials) of the semiconductor then we will have and

injection barrier for holes from the metal to the semiconductor. If the Fermi level is *lower* than the conduction band (LUMO level in organic materials) of the semiconductor then we will have an injection barrier for electrons from the metal to the semiconductor. In other cases, the barrier, which in semiconductor physics is called *Schottky barrier*, will not be present and we will have a *Ohmic contact*. Barriers up to 0.3 eV still are easily overcome thermally by charge carriers and we still have a Ohmic contact. This model ignores certain effects that happen at interfaces, such chemical reactions and forming of extra localized levels within the band gap.

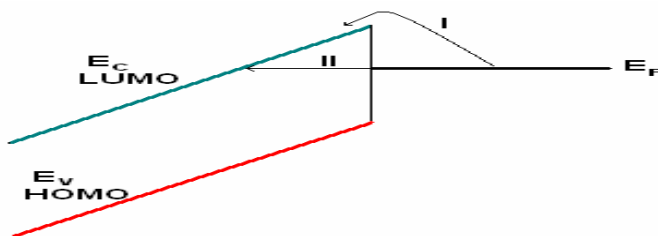


Fig. 8: Charge injection processes: thermionic emission (I) and tunneling (II)

Charge injection of charges occur by two major mechanisms. The first one is *thermionic emission* (Figure 8, process I), a process in which the energy of a charge has to be increased to go over the barrier. This process is thermally activated, similar to hopping transport, where thermal energy supplies the necessary energy for the charge to go over the barrier (if the barrier is low, i.e. in an Ohmic contact). This process is thus favored if the temperature of the system increases. The second process is *tunneling* across the potential barrier (Figure 8, process II). This process relies on the transfer probability between electronic wave-functions at (nearly) the same energy. Normally this process is independent of temperature, but depends strongly on the applied electric field since fields affect all the energy levels of the metal and the semiconductor. This phenomenon, thus, will become dominant at low temperature or high fields.

1.2– The field-effect transistor^{4, 18, 19}

The field-effect transistor (FET) is the one of the most used and important electronic components in modern electronics. The most used type of FET is the Metal-Insulator-Semiconductor FET or abbreviated MIS-FET. This type of FET has, like any transistor, three electrodes: the gate, isolated by an insulator, usually an oxide and the source and the drain which are in contact with the semiconductor. An organic semiconductor is usually spin-coated or evaporated on a FET, so the source and drain electrodes are either under the organic layer, on top of the insulating layer, or are put on top of the organic layer. We talk the of bottom and top contact FETs, respectively. A schematic picture of a bottom contact MIS-FET is given in Figure 9 below.

1.2.1- Basic working of the FET

The MIS-FET can be basically seen as a parallel plate capacitor, as can be deduced from Figure 9, where the gate electrode is isolated by an insulating layer, usually an oxide, from the conducting electrodes, the source and the drain, while the conducting electrodes make contact with the semiconductor (see Figure 9).

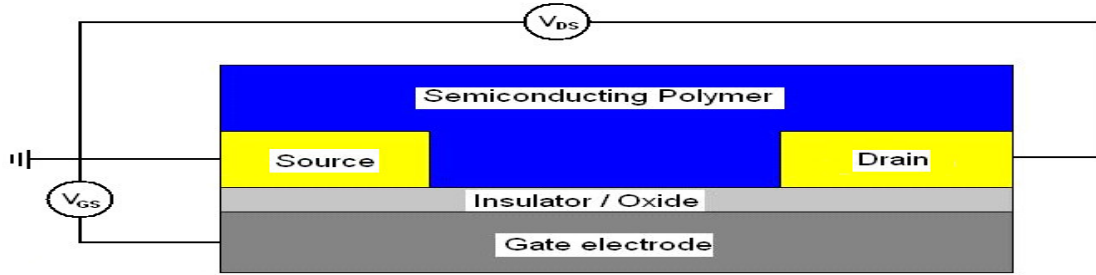


Fig. 9: Schematic cross section of a bottom contact MIS-FET, where the source acts as common ground.

To understand how a MIS-FET operates it is important to keep a close look on what happens at the semiconductor-insulator interface when different biases are applied to the metal with respect to a ground. We will discuss the case for a p-type semiconductor since most conjugated polymers are of this type. There are three possible cases. The first case is when the bias on the gate electrode (V_{GS}) is equal to the *flat-band* bias (V_{FB}). Then we will have a *flat-band* condition, where no band bending occurs and the Fermi levels of the semiconductor and the gate electrode are aligned. The only charge carriers present in the semiconductor are the carriers that occur by ‘natural’ means such as thermal excitation or doping (Figure 10a.).

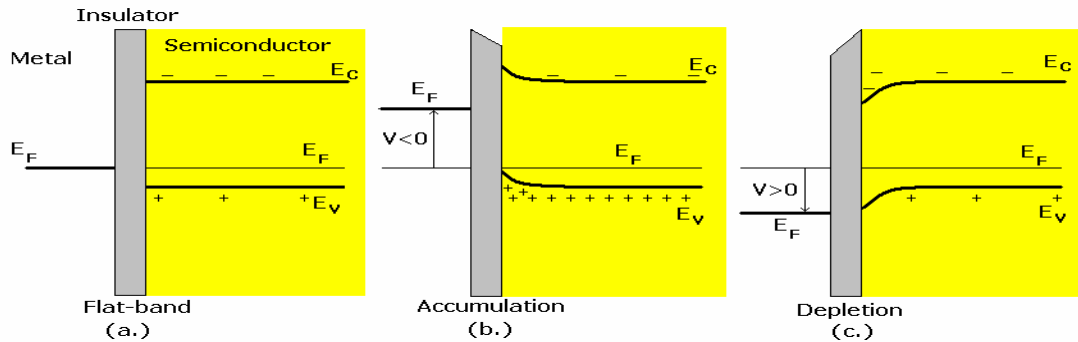


Fig. 10: Energy band diagram of an ideal Metal-Insulator-Semiconductor device with p-type semiconductor, similar to the gate-oxide-semiconductor structure in a MIS-FET. The picture depicts three situations: (a.) The Flat-band condition where there is no applied bias, hence no band-bending. (b.) The Accumulation condition where a negative bias is applied on the metal causing the bands of the semiconductor to bend ‘upwards’ which causes accumulation of holes at the semiconductor-insulator interface. (c.) Depletion condition where a positive bias is applied to the metal which causes a depletion of holes in the semiconductor.

The second case is when we apply a negative bias on the gate electrode (or more negative than V_{FB}), then its Fermi energy level will be raised. Consequently, the bands of the semiconductor will bend upwards in energy causing an accumulation of positive charges in the valence band at the interface to compensate for the negative charges on the gate (keeping in mind that the device is similar to a capacitor). This is the *accumulation* condition or regime (see Figure 10b). In this regime the accumulation of charges present at the interface with insulator form a *channel* between the source and gate electrode, allowing (hole) current to flow between them. This is called the *on-current*. This channel is usually a few nanometers thick and the charge density decreases exponentially with the distance from the semiconductor-insulator interface¹⁹.

The third case is when we apply a positive bias (or more positive than V_{FB} , Figure 10c) to the gate electrode. The Fermi level of the electrode will then be lowered, which is the reverse of the previous case: the bands of the semiconductor will be bent downwards causing a depletion of positive charges in the valence band and a slight accumulation of negative charges in the conduction band. This is called the *depletion* condition or regime. In this regime there will be a very low charge density, hence the current flow, called the *off-current*, between the source and the drain will be very low, usually several orders of magnitude lower than the on-current.

The switch-on voltage (V_{SO}) of a FET is defined as the flat-band voltage V_{FB} . This is the voltage that sets the boundary between the on and off state of the transistor. The transistor, as we can deduce is in the on state in the accumulation regime and the off state in the depletion regime. If the gate voltage is lower than the switch-on voltage then there will be no change in current in the channel between the source and the drain. Above V_{SO} however an increase in the gate voltage will also result in an increase of the current between the source and the drain. An important characteristic of the FET is also the *on/off ratio* which is defined as:

$$R_{ON/OFF} \equiv \frac{I_d(ON)}{I_d(OFF)} \quad (2)$$

Conjugated polymers can reach $R_{ON/OFF}$ values above 10^6 in a field-effect transistor.

1.2.2- The field-effect mobility²⁰⁻²²

In the accumulation regime of the gate voltage charges are induced in the semiconductor at the interface with the insulator creating a ‘channel’. If we apply a voltage V_{DS} between the drain and the source a current is induced in the channel. If the drain-source voltage is much lower than the gate voltage then the current will depend linearly on V_{DS} . This is called the *linear regime*. The current is described by:

$$I_{DS} = WC_i V_{GS} \mu_{FE} \frac{V_{DS}}{L} \quad (3)$$

where W is the width of the FET channel, L is the distance between the drain and the source, C_i the capacitance of the insulator layer and μ_{FE} is the field-effect mobility in the linear regime. The V_{GS} used in Eq. 3 is the gate voltage, corrected for the threshold voltage of the device. It is also important to note that $C_i V_{GS}$ is the total amount of accumulated charge and V_{DS}/L is the electric field in the channel. Equation 3 assumes that all the charges in the semiconductor have the same mobility. This is clearly not the case in a disordered organic semiconductor, so the μ_{FE} in equation 3 is the average mobility of the charge carriers. The mobility can be derived from equation 3 and can be calculated from the following relation:

$$\mu_{FE} = \frac{L}{WC_i V_{DS}} \left(\frac{\partial I_{DS}}{\partial V_{GS}} \right)_{V_{DS} \rightarrow 0} \quad (4)$$

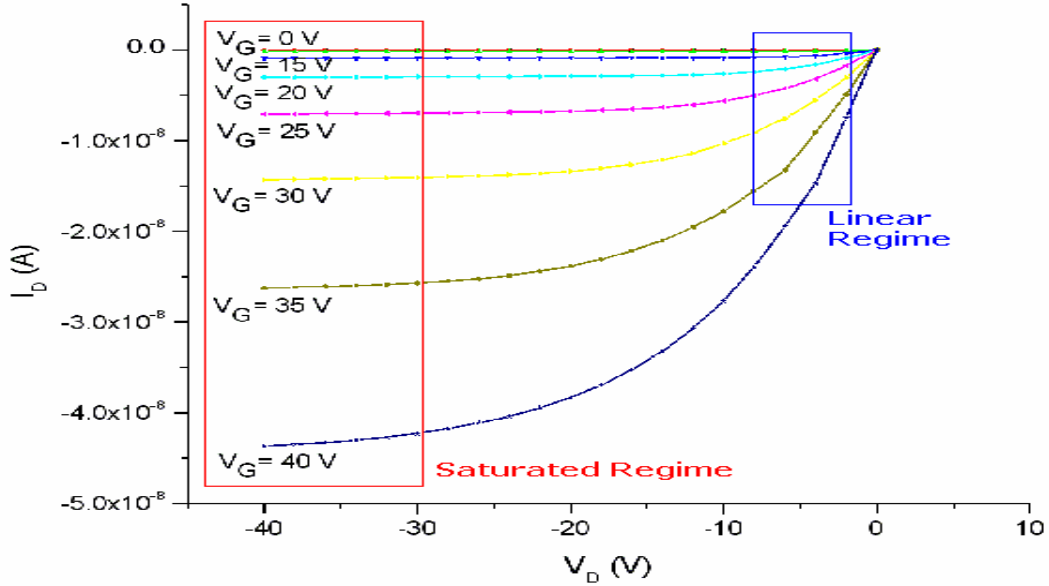
If we increase the drain-source voltage so that it comes closer to the gate voltage, the current is no more linearly dependent with the drain-source voltage anymore, as a matter of fact it becomes field independent and depends quadratically on the gate voltage as it is described in equation 5 below:

$$I_{D,Sat} = C_i \mu_{Sat} \frac{W}{2L} V_{GS}^2 \quad (5)$$

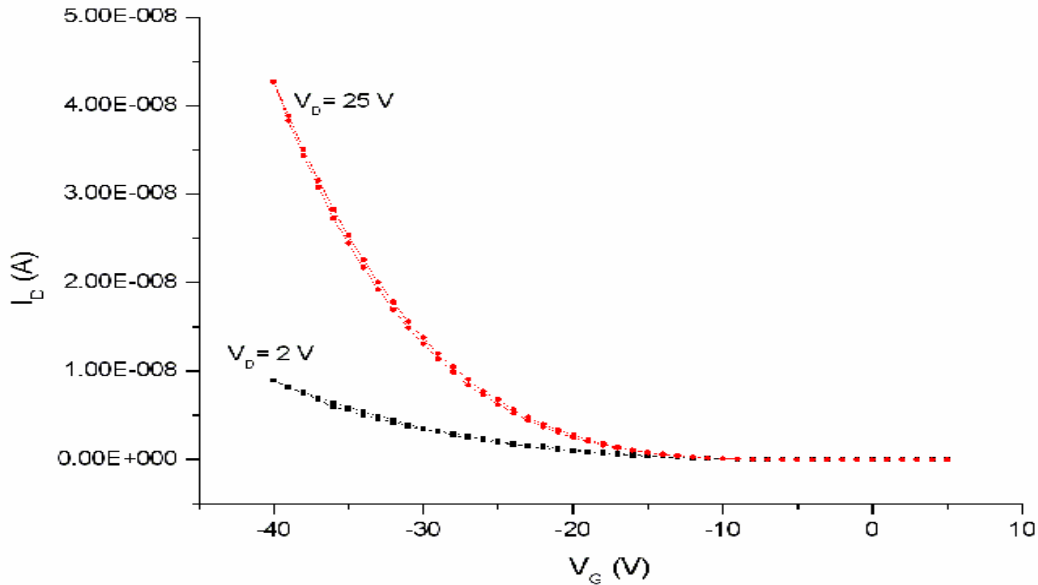
V_{GS} is the gate voltage corrected for the threshold voltage. Furthermore the mobility in the *saturation regime* μ_{Sat} is higher than the mobility in the linear regime. Rearranging equation 5 gives us the relation for the saturated mobility:

$$\mu_{Sat} = \frac{L}{2WC_i I_{D,Sat}} \left(\frac{\partial I_{D,Sat}}{\partial V_{GS}} \right)^2 \quad (6)$$

which as we can see from the equation above it depends quadratically on V_G .



a.



b.

Fig. 11: Current-voltage characteristics of a MIS-FET. (a.) Drain current versus drain-source voltage. Depicted are the linear regime at low V_D and the saturated regime at high V_D . (b.) Drain current versus gate voltage for two different drain-source voltages: one in the linear regime ($V_D = -2$ V) and one in the saturated regime ($V_D = -25$ V)

Problems arise if the contact between the metal electrodes and the polymer are not ohmic. In that case we shall have a contact resistance and the apparent mobility calculated with equation 4 will be lower (sometimes some orders of magnitude lower) than the real field-effect mobility in the material. The field-effect mobility, in presence of a contact resistance is also measured in the linear regime of the FET operation.. The linear portion of I_D-V_D is used to find R_{ON} , the total source-drain resistance, which is defined as:

$$R_{ON} \equiv \frac{\delta V_D}{\delta I_D} \quad (\text{in the linear regime}) \quad (7)$$

This is done for transistors with different channel lengths L . The values of R_{ON} are then plotted as a function of channel length and the slope of such a plot describes the channel resistance, R_{CH} , per unit channel length. The intercept of the plot (the extrapolated resistance of a device of zero channel length) gives R_S , the *total parasitic series resistance* of the source and drain contacts. The true field-effect mobility, μ_{FE} , may be inferred from the gate voltage dependence of the inverse of the slope of R_{ON} versus the channel length:

$$\frac{\delta \left[\left(\frac{\delta R_{ON}}{\delta L} \right)^{-1} \right]}{\delta V_G} = \mu_{FE}(V_G, T) W C_{OX} \quad (8)$$

where C_{OX} is the capacitance per unit area of the gate oxide and W is the width of the channel. So the field-effect mobility can be calculated:

$$\mu_{FE}(V_G, T) = \frac{1}{W C_{OX}} \frac{\delta \left[\left(\frac{\delta R_{ON}}{\delta L} \right)^{-1} \right]}{\delta V_G} \quad (9)$$

If the contacts between the electrodes and the material are ohmic, there will be no contact resistance and the mobilities calculated with equation 4 should be equal to those calculated with equations 9. If we use different transistors with different types of electrodes one should get by equation 9 always the same mobility for the same semiconducting material.

1.2.3- The effect of oxygen and water on the organic FET operation^{23,24}

Generally semi-conducting polymers and organic materials are unstable in air or can be easily doped by oxygen and water. The presence of air in the system changes the conducting characteristics of the semiconductor and influences the operation of an organic FET. Polymer and organic materials, due to their disordered nature are usually very porous so water and oxygen molecules are easily absorbed into the materials. Many polymers, such as polypyridine are unstable in air and are oxidized by oxygen or water, breaking the conjugation or trapping the free charges, reducing the conductivity of the organic semiconductor, sometimes rendering it non-conducting.

Other materials, such as polythiophenes are stable in air, meaning that these materials are not degraded in presence of oxygen or water, yet such materials are easily doped in air. The molecules, such as air, absorbed by the materials will usually be chemisorbed or physisorbed, thereby doping the semiconductor. The doping will increase the conductance of the semiconductor. In a FET the conduction between the drain and the

source will be improved due to the high density of free charges. The conduction will either be exponential depending on a power of V_{DS} , similar to conduction in LED where the current density J is proportional to $(V_{DS})^2$ or will even become ohmic-like, with linear dependence between the current and the voltage. The gate dependence will still present but becomes much weaker when the semiconductor is doped. Charges will still be accumulated at the semiconductor-insulator interface, yet the presence of dopants already produces a relatively high amount of free charges in the polymer. The effect of charge accumulation due to the gate bias will then be diminished. The effects of this type of doping are usually reversible, since the materials are doped but not chemically degraded. Materials which degrade in air do not recover after exposure to oxygen and water. Polymers such as polythiophenes are doped in a matter of seconds when exposed to air and its conduction becomes metallic-like as described above. Then, if we return polythiophenes into vacuum and optionally heat them, the oxygen and water will be released from the material which will become semi-conducting again.

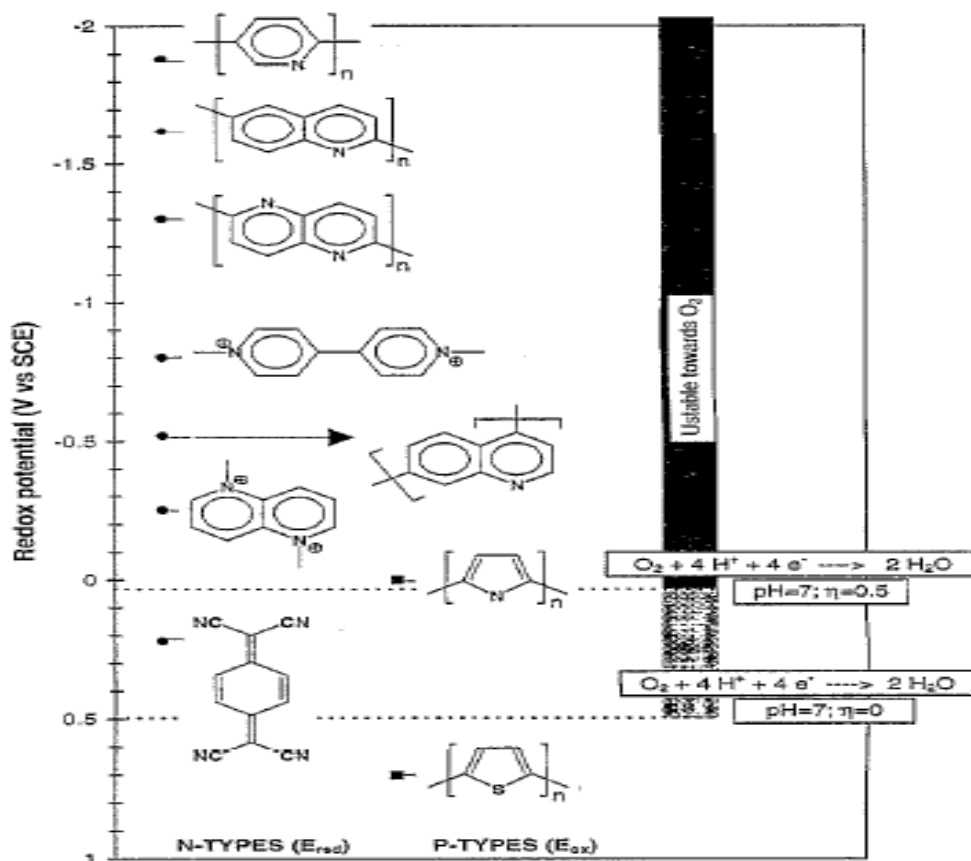


Fig. 12: Electrode potentials at which a few n-type conducting polymers and organic compounds can be reduced (solid circles) and electrode potentials at which two well-known p-type conducting polymers can be oxidized (solid squares). Included are only materials of which the stability under ambient conditions has been reported. (Figure from: De Leeuw et. al, *Synthetic Metals* (1997) 87 p56).

The property of some polymers of being stable in air and perhaps in water depends on their redox potential. The redox potential of semiconducting polymers is determined by

the energetic position of their HOMO levels. Polymers with a high redox potential have a HOMO which is very deep in energy compared the vacuum. Polythiophene for example has a HOMO which has an energy of about -5 eV compared with the vacuum, hence it has a high redox potential, around 5 V, as it is also shown in Figure 12 above, where as zero potential the saturated calomel electrode (SCE) was taken, which has a redox potential equal to +4.681 V (or + 0.241 V versus the standard hydrogen electrode). Polymers that have a redox potential lower than the SCE, hence can be reduced by the SCE in this figure, are unstable for oxygen. The reason is because the redox potential of molecular oxygen is higher than the HOMO levels of these materials and consequently the reaction with oxygen destroys the conjugation of the system. In Figure 12 such polymers are indicated with a black solid circle. On the other hand polymers that can be oxidized in the figure, indicated with a solid black square, are air stable. One of these polymers, as it can be seen, is (regioregular) polythiophene. These polymers are not affected by oxygen, as their HOMO levels are too deep in energy and their redox potentials are too high, hence they remain stable. It is important to note that even if some polymers are air-stable, such as polythiophenes, they are not necessarily unaffected by air as they can be reversibly doped by it as it was discussed above. Water stability entails a similar process, yet for a polymer to be water stable, an even higher redox potential is needed than for stability towards oxygen. Polythiophene for example is air stable, yet it is not water stable, as it is degraded by water.

1.3– Light-emitting diodes and hole-only devices²⁵

Light-emitting polymers were discovered only fifteen years ago in 1990, since then extensive research has been done on polymer light-emitting diodes (LED). The basic structure of a LED is depicted below in figure 13.

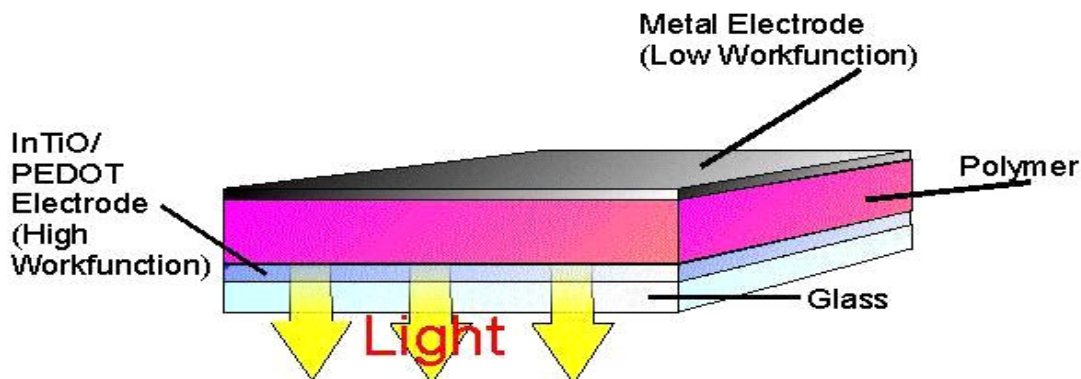


Fig 13: A schematic view of a light-emitting diode. A hole-only device has the same basic structure but a high work function metal is put on top of the semiconductor layer.

Three factors are important for the operation of LED. The first is the injection of charge from the electrodes into the semiconductor, which has already been discussed in paragraph 1.1.5, the second is charge transport through the semiconducting layer (discussed in paragraphs 1.1.2 to 1.1.4) and the third is the recombination of charges within the layer.

In the forward bias, holes and electrons are injected from the anode and the cathode respectively. The anode is formed by a high work function ($\phi \sim -5$ eV) conductor, such as Indium Tin Oxide (ITO), which is also transparent. The ITO is usually covered by PEDOT:PSS to improve wetting. Assuming an ohmic contact, the Fermi level will approximately coincide with the HOMO (π -level band) level of the semiconductor and under forward bias condition holes will be injected from the electrode into the HOMO. The cathode is usually a low work function ($\phi \sim -3$ eV) metal (Ba, Ca) covered by an air stable metal such as aluminum. Assuming an ohmic contact, the Fermi level of the electrode will approximately align with the (π^* -level band) LUMO level and under forward bias condition the cathode will inject electrons into the LUMO. The electrons and holes will then travel along the bulk of the material through the LUMO and HOMO bands, respectively, aided by hopping transport where the band structure is broken. The charge carriers will, at a certain point in the bulk, meet each other and recombine, releasing the energy in the form of electromagnetic radiation with energy roughly equal to the gap between the HOMO and the LUMO ('roughly' because the energy is not *exactly* equal to the HOMO-LUMO band gap, other factors such as exciton binding energy and exciton energy levels come into play, but this is not discuss here).

In an hole-only device or HOD, the current, as the name suggests, is transported only by holes and not by electrons. This device is very similar to LED, but instead of a low work function metal, a high work function metal (Au, Pd) is used as cathode. Electron injection will then be blocked and only holes will be injected in the HOMO of the semiconductor. In a HOD there will be almost no recombination since the LUMO is almost empty (of electrons) and, generally, a hole-only device won't emit any light.

The current in a LED or HOD, assuming the electrode/semiconductor contacts are ohmic, is space charge limited, hence limited by the bulk properties of the semiconductor. The space charge limited current density J_{SCL} (in Am^{-2}) in an hole-only device is quadratically dependent on the voltage V and has inverse cubic dependence with the layer semiconducting thickness L as described in equation (10) below:

$$J_{SCL}(V, L) = \frac{9}{8} \epsilon \mu \frac{V^2}{L^3} \quad (10)$$

The mobility μ for the holes is obtained by fitting with equation (10) the data obtained from experiments. The ϵ in the equation is the dielectric constant $\epsilon = \epsilon_r \epsilon_0$ where ϵ_r is usually assumed to be $\sim 2-5$ for conjugated polymers. At high fields the relationship given in (10) will no longer be valid and the current J will deviate becoming exponentially dependent on the square root of the field ($E = V/L$) as given in equation (11) below.

$$J(V, L) = \frac{9}{8} \epsilon \mu \frac{V^2}{L^3} \exp\left(\gamma \cdot \sqrt{\frac{V}{L}}\right) = J_{SCL} \cdot \exp\left(\gamma \cdot \sqrt{\frac{V}{L}}\right) \quad (11)$$

The γ that appears in equation **11** is a fit parameter.

The measurement of electron current must be performed on electron-only devices, which are more difficult to fabricate and will not be discussed in this project since the main focus here is on hole mobilities.

1.4– Aim of this research

Many applications of semiconducting polymers, such as acting as active layers in biosensors, require that a polymer should be stable in air and in water, which means it should be stable in presence of O₂ and H₂O. This stability should not be only a chemical stability, i.e., that the polymer material remains intact under the influence of the agents named above, but it should also possess ‘operational stability’, i.e., that the current-voltage (I/V) characteristics of a device with a polymer active layer should be stable even in the presence of oxygen and water. Polymers such as P3HT are air stable, their chemical structure is not compromised by oxygen, yet P3HT is very quickly doped by molecular oxygen and in a matter of seconds the normal I/V characteristics of a FET with P3HT as active layer disappears. We investigated in this report a novel polyfluorene diamine polymer comparing it to values in the literature for similar materials and to P3HT. The influence of oxygen and water in time will be observed.

2 - Materials and methods

2.1 – Chemicals and materials

Cleaning solvents: acetone, toluene, propane-2-ol (*iso*-propanol).

Solvents for the polymers: toluene, 1,2-dichlorobenzene, chloroform.

All the chemicals used were purchased from Sigma, Aldrich and Merck.

The polymers used for the FET, the HOD and the LED were: Poly(3-Hexyl)thiophene, regioregular (Figure 14a) abbreviated to RR-P3HT and Polyfluorene tetraphenylene diamine (PFTPDA) which is shown in figure 14b. The polymers were synthesized by Jurjen Wildeman.

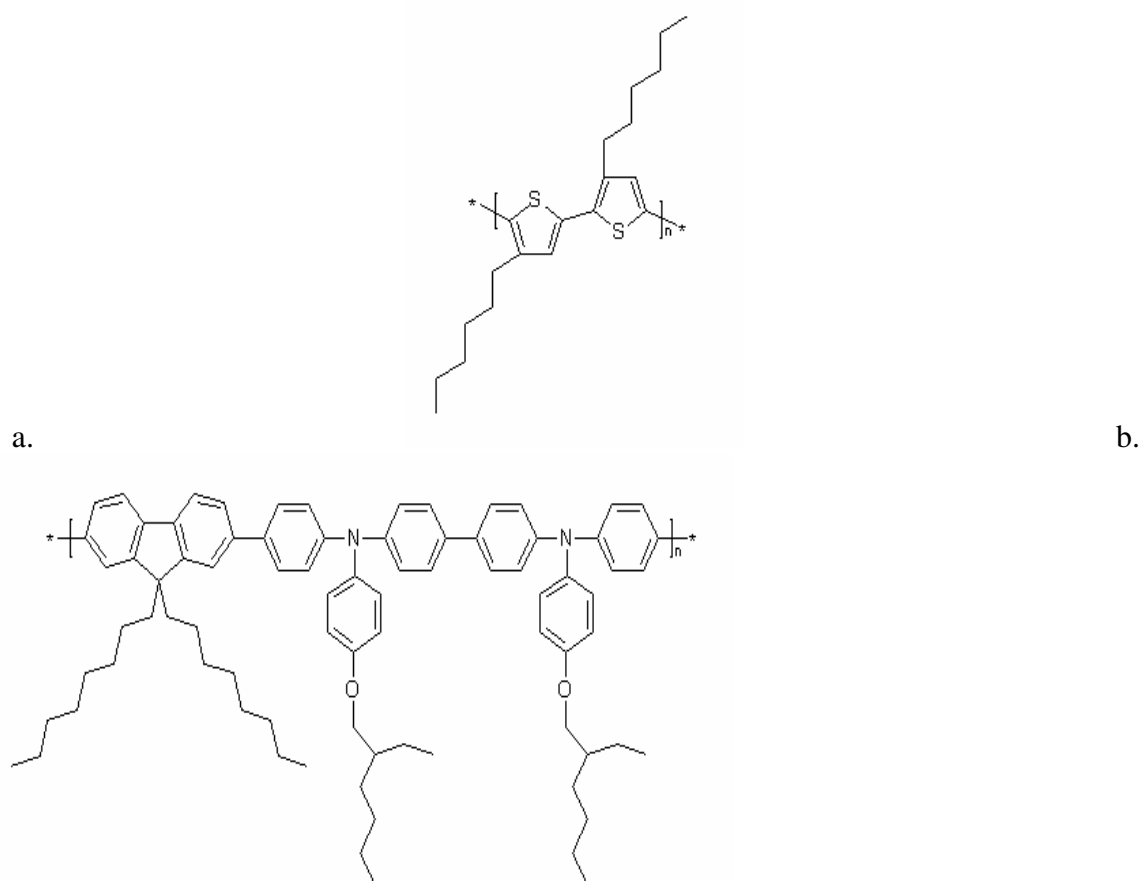


Fig. 14: a. Poly(3-Hexyl)thiophene, regioregular (RR-P3HT); b. Polyfluorene tetraphenylene diamine (PFTPDA)

2.2 – Sample preparation

2.2.1 – Preparation of polymer solutions

Regioregular poly-3-hexylthiophene (RR-P3HT) was dissolved in chloroform (CHCl_3) at a certain concentration and stirred at ~500 rpm at room temperature, overnight before spincoating. The concentration used varied between 1 and 2 mg/ml.

Polyfluorene-tetraphenyl-diamine (PFTPDA) was dissolved in toluene at a concentration of 20 mg/ml and stirred at ~500 rpm at room temperature overnight. Then the polymer was filtered with a 5.0 μm filter and put at 60-70 °C to stir at ~500 rpm before spincoating. All solutions were prepared under nitrogen atmosphere in the glove-box.

2.2.2 – Preparation of thin-film transistors

The thin-film transistors were prepared on pre-made 2×2 cm substrates obtained from Philips, made from highly doped silicon with a layer of 200 nm thermally oxidized SiO_2 . Photolithography was used to pattern gold source and drain electrodes on top of the oxide layer. The oxide layer was also treated with the hexamethyldisilane (HMDS) primer to render the oxide surface hydrophobic for better wetting and to reduce the formation of trapped charges at the interface between oxide and semiconductor. The substrates were cleaned first by rinsing them with acetone and then with propane-2-ol (*iso*-propanol) and then spin-dried. Under nitrogen atmosphere, in the glove-box, the cleaned substrates were spincoated. First they were rotated at low speed (400 rpm) for a few seconds while the polymer solution was dropped on the surface of the substrate, then the speed was increased (= 1000 rpm) and the substrate was rotated for 30 to 60 seconds, obtaining thin polymer films (=200 nm) on top of the oxide and the source-drain electrodes. RR-P3HT was spincoated at room temperature and the polymer solution (in chloroform) was not filtered. The PFTPDA solution in toluene was heated at 60-70°C, after it was filtered with a 5.0 μm filter, before spincoating.

2.2.3 – Preparation of LED and HOD

Glass substrates with a patterned layer of ITO (InTiO) electrodes were cleaned by scrubbing them for approximately 5 minutes with 10% detergent (Extran MA 02 Neutral, purchased from Merck) solution in de-mineralized water at ~60°C. The substrates were rinsed with de-mineralized water, put in ultrasonic bath in acetone, rinsed again with de-mineralized water, put in ultrasonic bath in *iso*-propanol and then spin-dried. The substrates were dried at 140°C for ten minutes in an oven and successively cleaned with UV/ozon for 20 minutes to remove any trace of organic materials on the glass and ITO and increase the ITO work function for better hole injection. In order to improve the performance and the stability of the device PEDOT:PSS was spincoated upon the substrate. This polymer acts as a transparent electrode with relatively high conductivity and high work function (~ 5.2 eV) and improves the wetting between the organic active layer and the ITO electrode. PEDOT:PSS consists of polyethylenedioxythiophene (PEDOT) doped with polystyrenesulfonate (PSS). Since we used low ohmic PEDOT:PSS the doping level was high. PEDOT:PSS was filtered with a 0.45 μm filter before spincoating. First PEDOT:PSS was added to the substrate then it was spun at 400 rpm

for 5 seconds and then at 1500 rpm for 40 seconds. The PEDOT:PSS films obtained were approximately 60 nm thick. The PEDOT:PSS was dried and annealed in the oven at 150°C for 10 minutes. The substrates were then transferred into the glove-box under nitrogen atmosphere, free of water and oxygen, and the PFTPDA polymer was spincoated on top of the PEDOT:PSS layer. The polymer was first put on top of the substrate then it was spun at 400 rpm for 4 seconds and then at 1000 rpm for 40 seconds. The spincoating procedure was performed with the lid of the spincoater open. The polymer film that was obtained was approximately 190 nm thick.

After the deposition of the polymer on the substrate the metal electrodes were evaporated on top, through a shadow mask. Electrodes of 50 nm gold were evaporated at high rate for hole-only devices (HOD), while electrodes of 20 nm samarium covered by 80 nm aluminum were evaporated for light-emitting diodes (LED). Evaporation was performed at high vacuum ($\sim 10^{-6}$ mbar)

2.3 – Measurements

2.3.1 – FET measurements

The thin-film transistors were measured with the Keithley 4200 Semiconductor Characterization System. The oxide layer on top of the gate was scratched away to uncover the doped silicon gate electrode and silver paint was put on the scratched surface to improve contact. Each probe electrode was put into contact with the transistor's electrodes by piercing through the semiconductor film and making direct contact with the electrodes. In the measurement the source was the common ground for the device. All measurements (if not specifies otherwise) were performed in vacuum (10^{-6} – 10^{-7} mbar) and in the dark. Two types of electrical measurements were performed: Output characteristics (I_D vs. V_D) and transfer characteristics (I_D vs. V_G). The measurements were repeated for different transistors, usually ring-transistors and sometimes finger transistors with different length/width ratio.

2.3.2 – LED and HOD measurements

The LED and HOD were measured under nitrogen atmosphere and in the dark. The Keithley 2400 Source Meter was used to measure the I/V-characteristics and the Keithley 6514 System Electrometer was used to measure the light output of the devices. The devices were scanned from zero volts bias to the maximum positive bias and then swept back to the maximum negative bias and then back to zero. The measurements were performed for LED or HOD with different areas, ranging from 10^{-5} to 10^{-4} m².

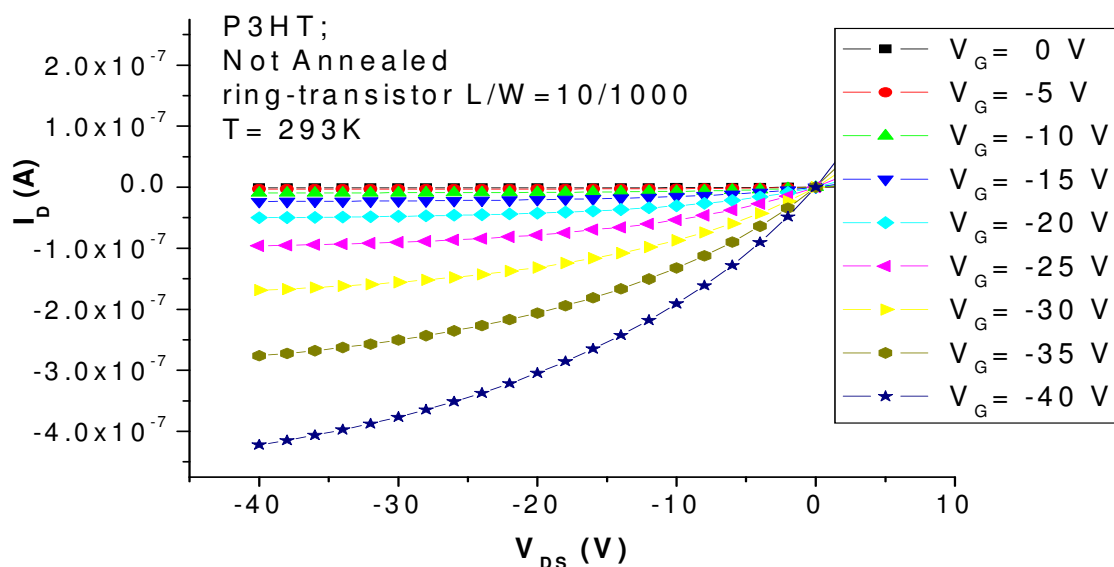
2.3.3 – Thickness measurements

The thickness of the polymer films in the LEDs, HODs and thin-film transistors were measured with the DEKTAK Profile Analyzer. Using a surgical knife, cuts were made on the polymer film to be analyzed, removing along a line the polymer material from the surface of the glass or the pre-made transistor chip. The stylus of the DEKTAK was lowered on the surface of the polymer nearby a cut and then the surface was scanned. The difference in height between the polymer surface and the surface from where the polymer was removed was measured.

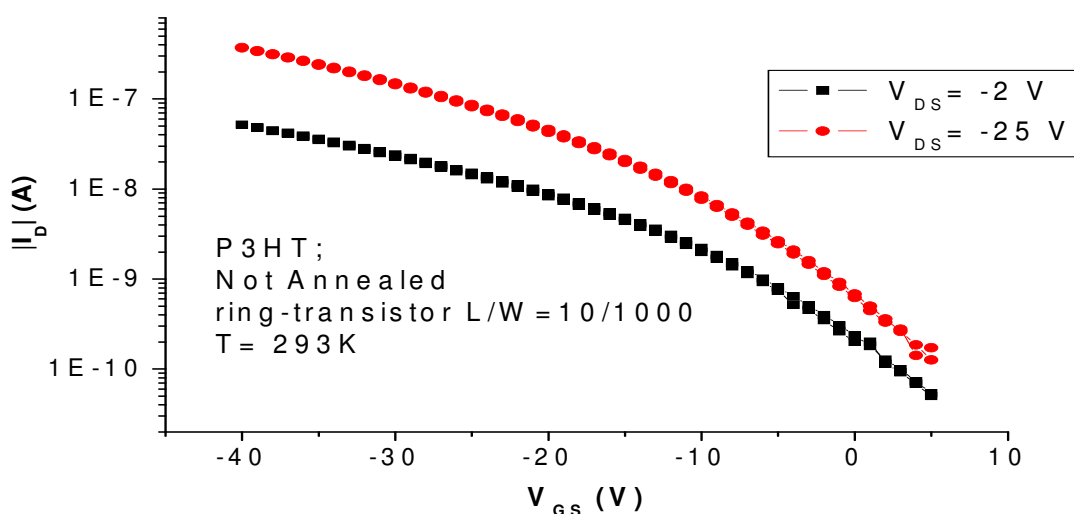
3 - Results

3.1 - P3HT and PFTPDA in vacuum

Measurements on the RR-P3HT and PFTPDA were performed in vacuum, where no oxygen or water can deteriorate or dope the polymers. In this manner the characteristics of the ‘pristine’ polymers could be investigated and quantified. The results for P3HT in vacuum and in absence of light are shown in Figure 15 below.



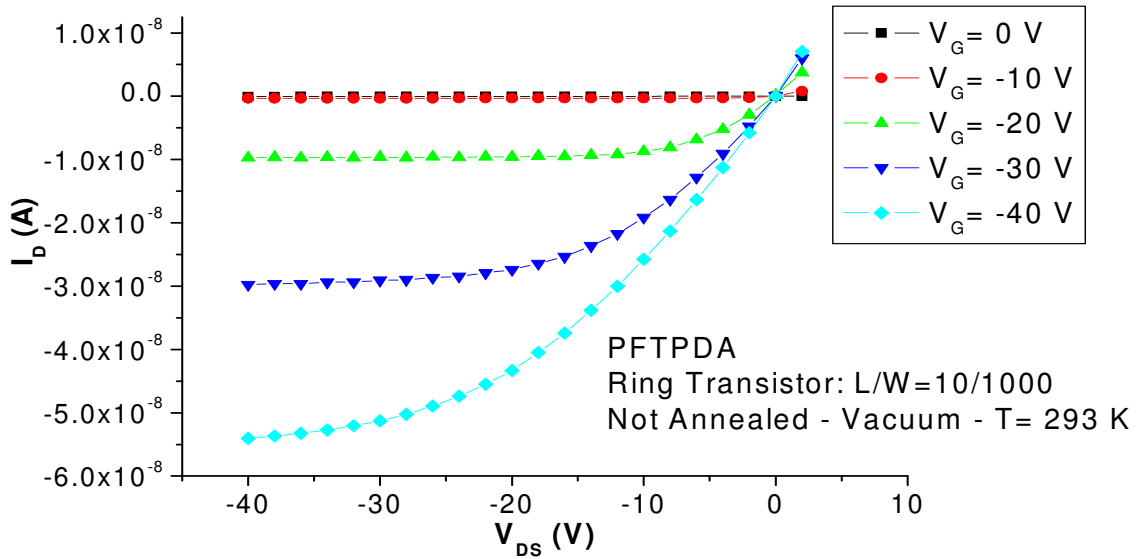
a.



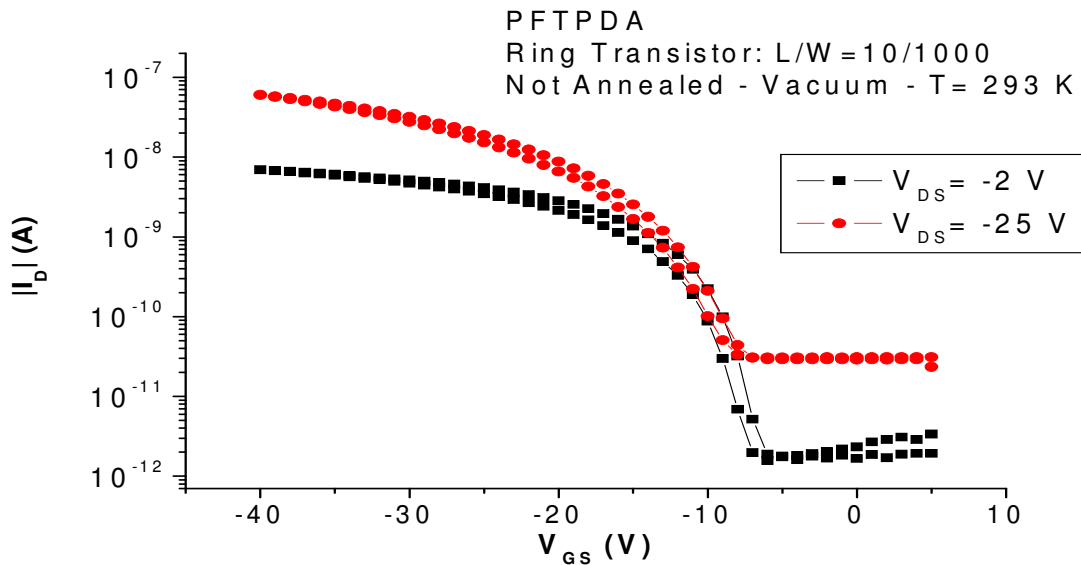
b.

Fig. 15: I/V -characteristics of a FET with unannealed region regular poly(3-hexyl)thiophene (RR-P3HT) as active layer. a). the drain current I_D versus the drain-source voltage V_{DS} at different gate voltages. b). the absolute value of the drain current versus the gate-source voltage V_{GS} at two different drain-source voltage values. The polymer was spincoated from a chloroform solution at a concentration of 1 mg/ml, 4 s at 400 rpm and 40 s at 1000 rpm.

In Figure 16 the same characteristics are shown for PFTPDA.



a.



b.

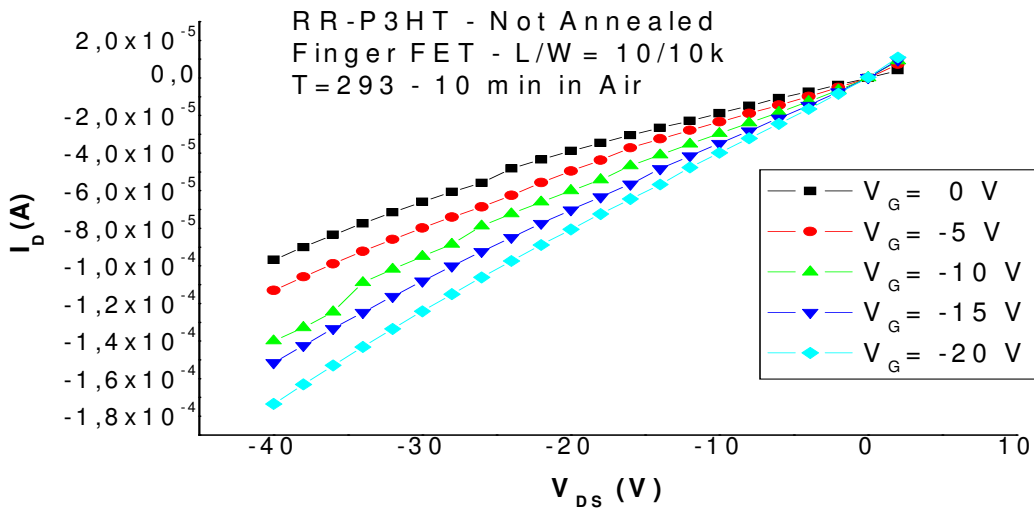
Fig. 16: I/V -characteristics of a FET with unannealed polyfluorene tetraphenylene diamine (PFTPDA) as active layer. a). the drain current I_D versus the drain-source voltage V_{DS} at different gate voltages. b). the absolute value of the drain current versus the gate-source voltage V_{GS} at two different drain-source voltage values. The polymer was spincoated from a toluene solution at a concentration of 20 mg/ml, 4 s at 400 rpm and 40 s at 1000 rpm.

The results presented in the two figures above reflect the common FET behavior as it is described in the introduction, with the I/V characteristics showing a linear and saturation regime in the I_D/V_{DS} mode. As it can be seen all I/V characteristics in this mode start at $V_{DS}=0$ V for both polymers, indicating that the threshold voltage V_{TH} of both polymers is equal to zero. The I_D/V_{GS} characteristics gives us two essential pieces of information

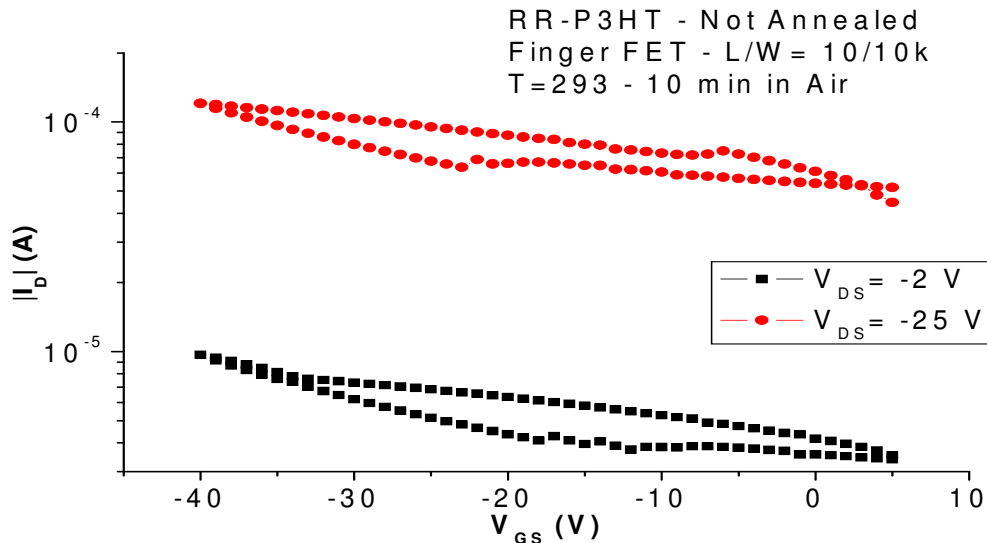
about the polymers. The first one is the switch-on voltage V_{SO} , the voltage at flat-band condition, the point at which the FET actually switches on. The V_{SO} of RR-P3HT is lower than zero as it can be seen in Figure 14b, meaning that at zero gate voltage the FET is already slightly in accumulation mode. It is different for the PFTPDA polymer, its V_{SO} is around -7 V gate voltage, under that voltage value no current is detected. The ON/OFF ratio of the currents of both polymers in vacuum was about 10^3 - 10^4

3.2 - P3HT and PFTPDA under the influence of air

The air present in our atmosphere is mainly composed of nitrogen (78%) and oxygen (21%) and the remaining 1% is composed of other gasses. Elements in the atmosphere and especially oxygen can affect the stability and performance of a polymer semiconductor as it was described in paragraph 1.2.3. We show here the effect of air on RR-P3HT and PFTPDA. Figure 17 shows the results from a FET with RR-P3HT as active layer exposed to air for 10 min. The effect of air on P3HT is very fast. The polymer film is quickly doped by oxygen increasing the charge carriers in the material, hence increasing the current. Figure 17a. shows that the dependence of the current towards V_{DS} is 'diode-like', the shape of the curve does not present a linear regime and at higher biases it does not bend and flatten to constant value as in a usual FET I/V-characteristic. The I_D/V_{DS} -characteristics appears to be similar to the space charge limited current that is measured in light-emitting diodes, probably signifying a high density of charges in the material due to the doping by oxygen. The mobility could not be calculated, since the characteristics do not comply with the model that produces equation 4 or equation 9, since the characteristic lacks a linear regime. We can also see from Figure 16b that the transistor does not really present an OFF and an ON mode and the ratio of the currents at $V_{GS} = -40$ V and $V_{GS} = 0$ V is lower than a factor 10, which is actually lower than the signal-to-noise ratio. The doping caused by molecular oxygen in RR-P3HT is fully reversible. If a sample is put back in high vacuum ($\sim 10^{-6}$ mbar) the polymer material is fully 'degassed' restoring the properties of the semiconductor, hence bringing the I/V-characteristics of the FET back to normal. Heating at low temperature ($\sim 40^\circ\text{C}$) for a few minutes speeds up and improves the degassing step.



a.

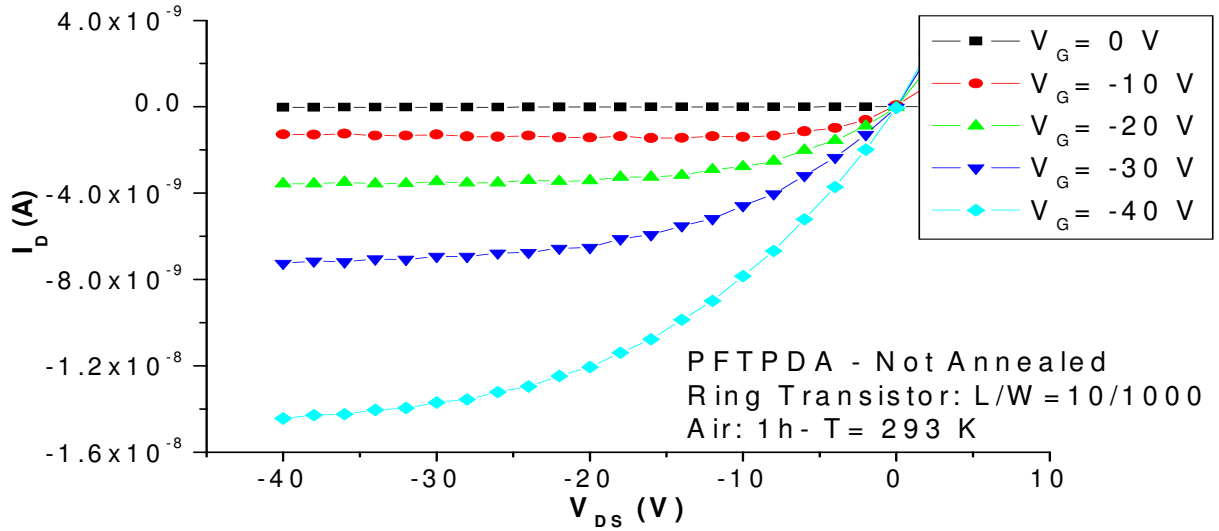


b.

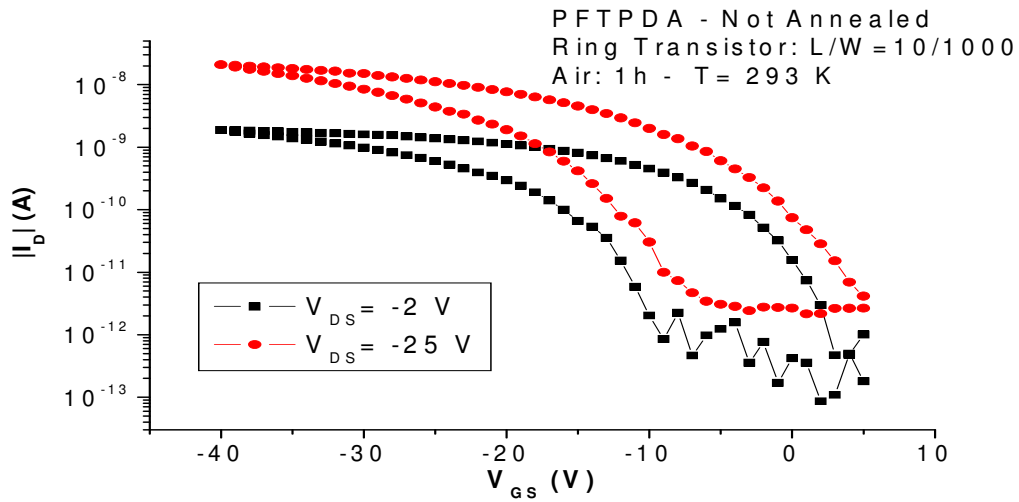
Fig. 17: *I/V*-characteristics of a finger FET with unannealed RR-P3HT as active layer after being exposed for 10 minutes in air. a) I_D versus V_{DS} at different gate voltages. b) the absolute value of the drain current versus V_{GS} at two different drain-source voltage values. The polymer was spincoated from a chlorobenzene solution at a concentration of 1 mg/ml, 4 s at 400 rpm and 40 s at 1000 rpm.

Figures 18 and 19 show the results of FET with PFTPDA as active layer measured (in air) after being exposed to air for a certain time. Figure 18 gives the *I/V*-characteristics of the FET measured after an exposure of one hour to air. Comparing the data with the one presented in Figure 16 we can see that after one hour in air the FET still retains the typical transistor characteristics, although the current is lowered about a factor 4 and the I_D/V_{GS} characteristics presents a strong hysteresis. In the forward sweep of the gate voltage we can see that V_{SO} is lowered and has now a value of about +6 V, yet in the back sweep the V_{Soff} (which is the voltage when the current returns to the off state) is -10

V. The ON/OFF ratio of the current, although lowered by a factor 10, is still quite high and approximately 10^3 .



a.



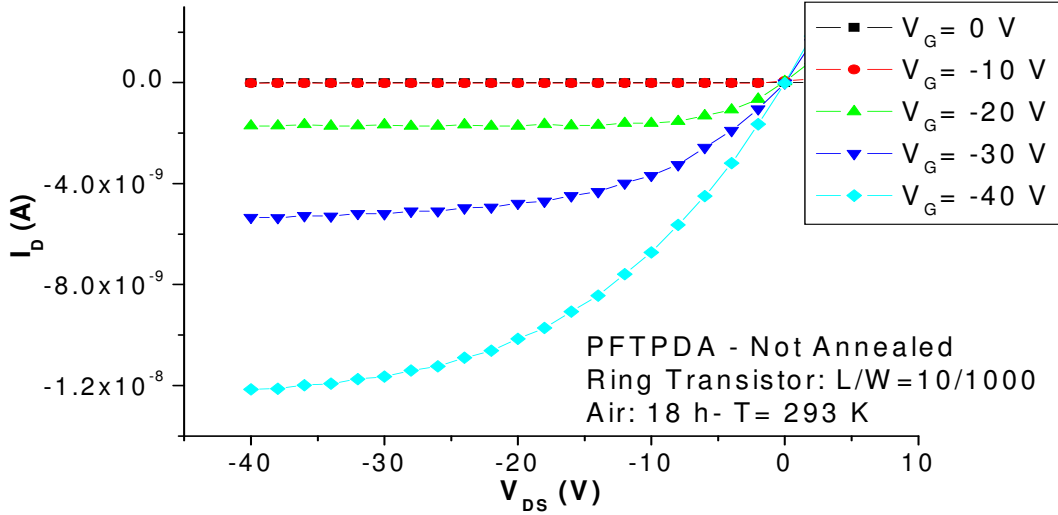
b.

Fig. 18: I/V -characteristics of a FET with unannealed PFTPDA as active layer after being exposed for 1 hour to air. a) I_D versus V_{DS} at different gate voltages. b) the absolute value of the drain current versus V_{GS} at two different drain-source voltage values. The polymer was spincoated from a toluene solution at a concentration of 20 mg/ml, 4 s at 400 rpm and 40 s at 1000 rpm.

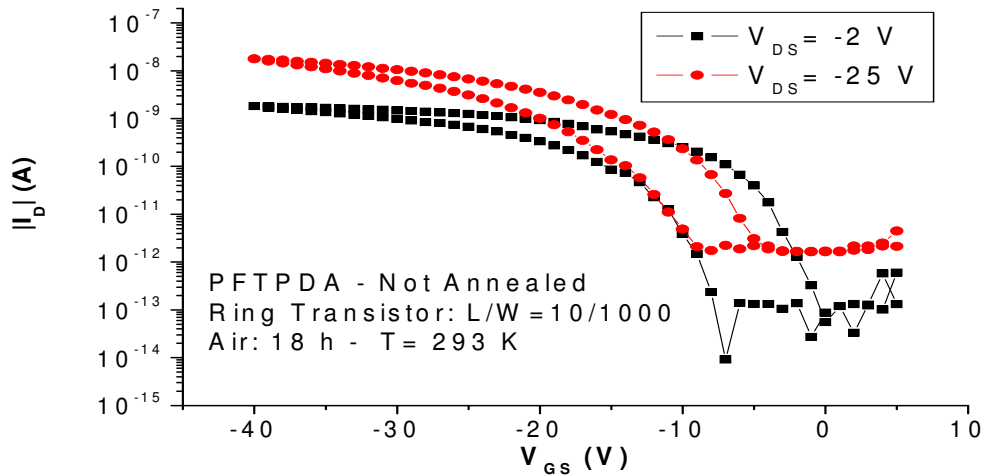
A further exposure to air is shown in Figure 19 which depicts the data for a FET exposed to air for at least 18 hours. Even after such relatively long exposure the FET retains the typical transistor characteristics with a linear and saturated regime. The current is only slightly lower than the current measured after only one hour of exposure to air. The I_D/V_{GS} of the FET actually improves after a longer exposure to air. The hysteresis is reduced compared to the hysteresis given by the data in Figure 19. The V_{SO} lowers to around zero volt for lower drain voltages and the V_{SOFF} remains approximately –

6 V as before. The ON/OFF ratio of the FET also improves at further exposure, and returns in the order of about 10^4 .

These results clearly show a good stability in air compared to materials like P3HT, which are quickly doped under influence of oxygen or like PPV's which react with molecular oxygen and are irreversibly degraded.



a.



b.

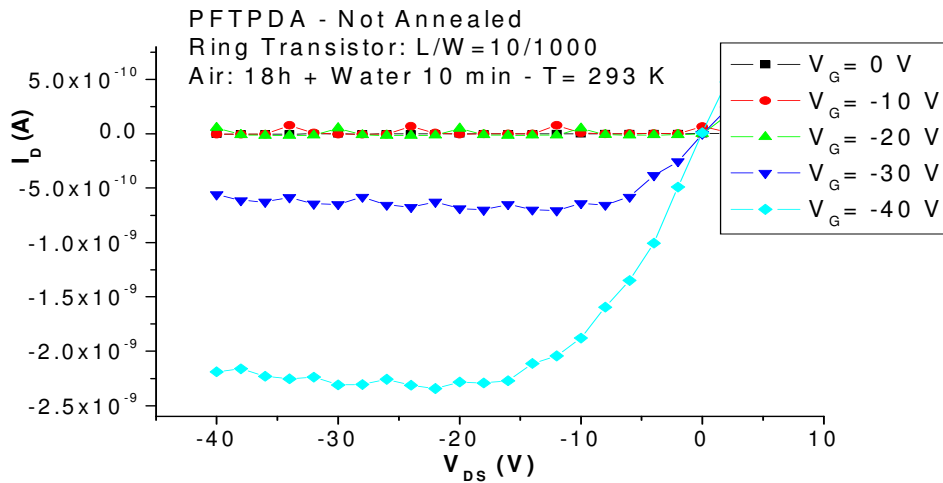
Fig. 19: *IV*-characteristics of a FET with unannealed PFTPDA as active layer after being exposed for 18 hours to air. a) I_D versus V_{DS} at different gate voltages. b) the absolute value of the drain current versus V_{GS} at two different drain-source voltage values. The polymer was spincoated from a toluene solution at a concentration of 20 mg/ml, 4 s at 400 rpm and 40 s at 1000 rpm.

The stability of PFTPDA does not hold in definitively, however. Samples measured after more than 72 hours of exposure in air showed erratic I_D/V_{DS} characteristics, with high noise, totally disrupting the normal transistor characteristics observed previously. Heating after putting the samples back in high vacuum restores PFTPDA to its original condition similar to P3HT, although it takes a longer time for PFTPDA to be degassed

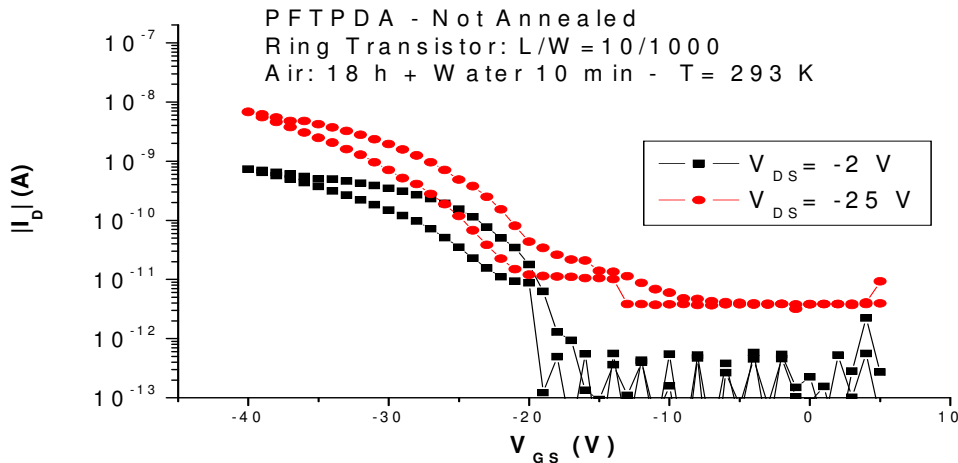
and de-doped than P3HT. P3HT usually is restored in a matter of minutes, while PFTPDA takes several hours.

3.3 - P3HT and PFTPDA under the influence of water

After 18 hours of exposure in air a PFTPDA FET sample was exposed to distilled water for 10 minutes, and afterwards the water was removed. The I/V characteristics were then measured in air. The results are shown in Figure 20. Even after being in contact for several hours with oxygen and being in direct contact with water, as seen in Figure 20, the PFTPDA polymer in the FET still retains somewhat the typical transistor characteristics although the current is strongly lowered, the ON/OFF ratio becomes lower than 10^3 and the V_{SO} is shifted to -20 V. Water clearly influences the FET performance negatively.



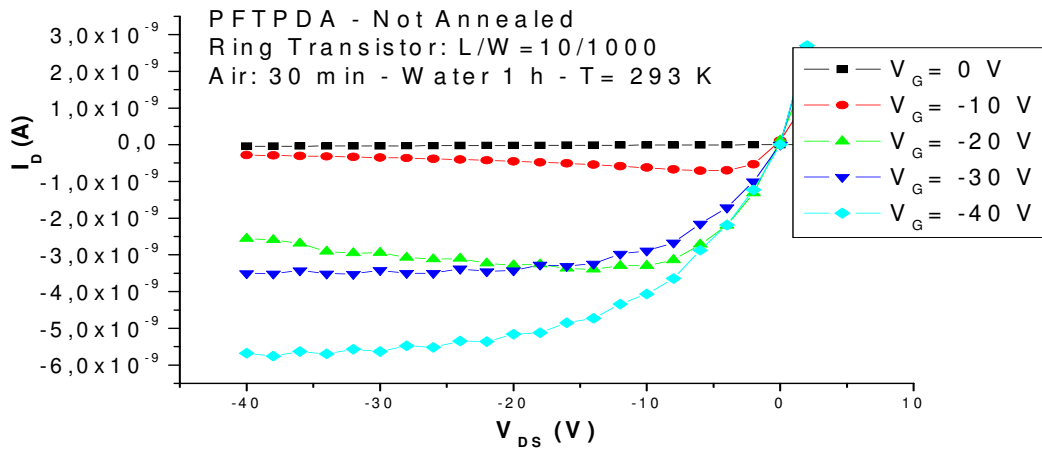
a.



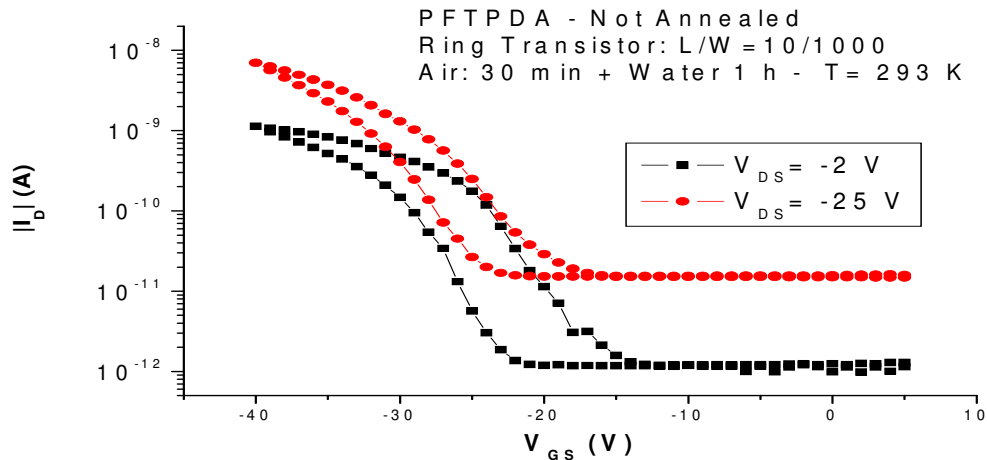
b.

Fig. 20: I/V-characteristics of a FET with unannealed PFTPDA as active layer after being exposed for 18 hours to air and 10 minutes to water. a) I_D versus V_{DS} at different gate voltages. b) the absolute value of the drain current versus V_{GS} at two different drain-source voltage values. The polymer was spincoated from a toluene solution at a concentration of 20 mg/ml, 4 s at 400 rpm and 40 s at 1000 rpm.

Another sample with PFTPDA as active layer was exposed only 30 min to air and then put into contact with distilled water for one hour. Afterwards the water was removed and the FET was measured. The results are shown in Figure 21. The influence of water on the polymer that was affected by oxygen only for a relatively brief time is not very different than for the results described above. The current is also lowered to very low values, about two orders of magnitude lower than the current in vacuum, and the FET still retains the typical transistor characteristics although, some strange behavior occurs in the saturated regions of the curves. The ON/OFF ratio is also lowered to less than a factor 10^3 . The I_D/V_{GS} characteristics present hysteresis and V_{SO} and the V_{SOff} are shifted and are approximately -10 V and -20 V, respectively.



a.



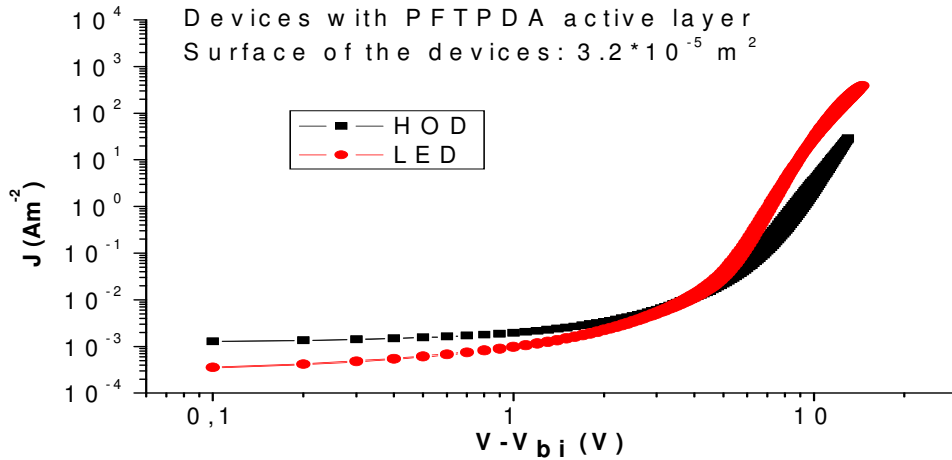
b.

Fig. 21: I/V -characteristics of a FET with unannealed PFTPDA as active layer after being exposed for 30 minutes to air and 1 hour to water. a) I_D versus V_{DS} at different gate voltages. b) the absolute value of the drain current versus V_{GS} at two different drain-source voltage values. The polymer was spincoated from a toluene solution at a concentration of 20 mg/ml, 4 s at 400 rpm and 40 s at 1000 rpm.

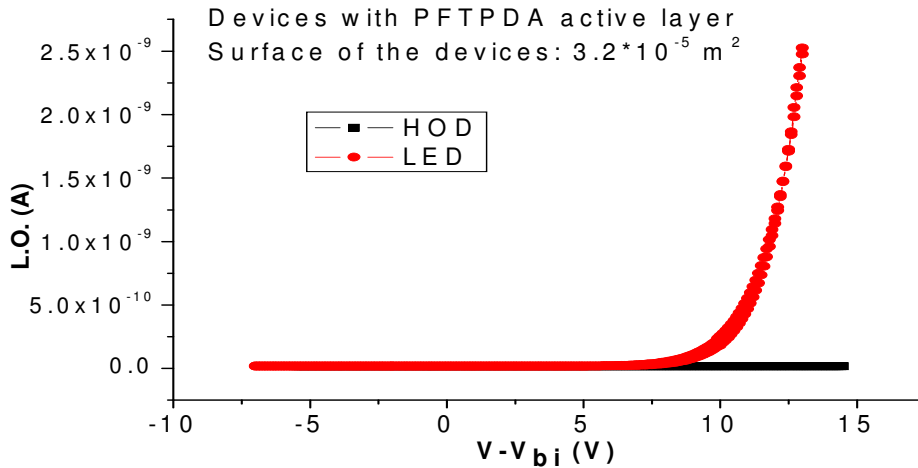
FET exposed to water could afterwards not be fully restored to their original functionality, even after being put in vacuum again and warmed up to ‘degas’ the polymer material. Unlike oxygen, water had a more permanent effect on both RR-P3HT and PFTPDA, reducing irreversibly their performance.

3.4 – PFTPDA Light-Emitting Diodes

To investigate further the properties of PFTPDA, hole-only devices (HOD) and light-emitting diodes (LED) were made and their I/V characteristics and light output was measured. The results from the measurements are shown in Figure 22.



a.



b.

Fig. 22: a. Current density J of HOD and LED with a unannealed PFTPDA as active layer versus the voltage corrected for the built-in voltage V_{bi} . The thickness of the polymer layer is equal to 190 nm for both devices. b. The light output of the devices (in terms of photocurrent produced by the light detector). The V_{bi} are -0.5V and -2V for the HOD and the LED respectively. The polymer was spincoated on the devices from a toluene solution at a concentration of 20 mg/ml, 4 s at 400 rpm and 40 s at 1000 rpm.

The currents measured in both the HOD and the LED could not be fitted with equation (10). Looking at Figure 22a. the first part of the graph of J is linearly dependent with the voltage signifying leakage, the second part (after approximately 4 V) could not be fitted with the relation for the SCL current. The relation between J and V could only be (poorly) fitted with equation 11 or by fitting the current density with a power of the voltage higher than 2 ($J \sim V^6$). The results clearly show that the current is not space charge limited as one would expect from a LED or a HOD, but has a higher power relation to the voltage, probably signifying traps in the material. The light output of the LED is not very high, as it can be seen in Figure 22b. The light emitted is blue shifted and has a maximum around 500 nm.

3.5 – Mobility data from the measurements

Using equation 4 and checking the result using equation 9 the field-effect mobility of the polymers was calculated from the I_D/V_{GS} characteristic measured for the FET in different conditions. Table 1 below summarizes the results from the calculations and gives the graphically extrapolated values for the V_{SO} and the V_{SOFF} .

Table 1: Results from FET made with two different polymers as active layer: RR-P3HT and PFTPDA. The threshold voltage V_{TH} and the switch-on voltage V_{SO} were determined from the graphs shown in Figures 14 to 20. The field-effect mobility of the polymers was calculated in the linear regime at $V_{DS} = -2$ V and $V_{GS} = -30$ V. The mobility is the mobility of the holes in the materials since it is a p-type semiconductor and the injection of electrons is hindered by using only gold electrodes with a high work function.

	RR-P3HT (vacuum)	PFTPDA (Vacuum)	PFTPDA (Air 1h)	PFTPDA (Air 18 h)	PFTPDA (Air 18 h Water 10')	PFTPDA (Air 30' Water 1h)
V_{TH} (V)	0	0	0	0	0	0
V_{SO} (V)	> +8	-7	+5	0	-20	-12
V_{SOFF} (V)	> +8	-7	-10	-7	-20	-20
μ_{FE} ($\text{cm}^2\text{V}^{-1}\text{s}^{-1}$)	8.51×10^{-4}	5.50×10^{-5}	1.58×10^{-5}	1.54×10^{-5}	6.92×10^{-6}	1.50×10^{-5}
I_{ON}/I_{OFF}	10^4	10^4	10^3	10^4	$< 10^3$	$< 10^3$

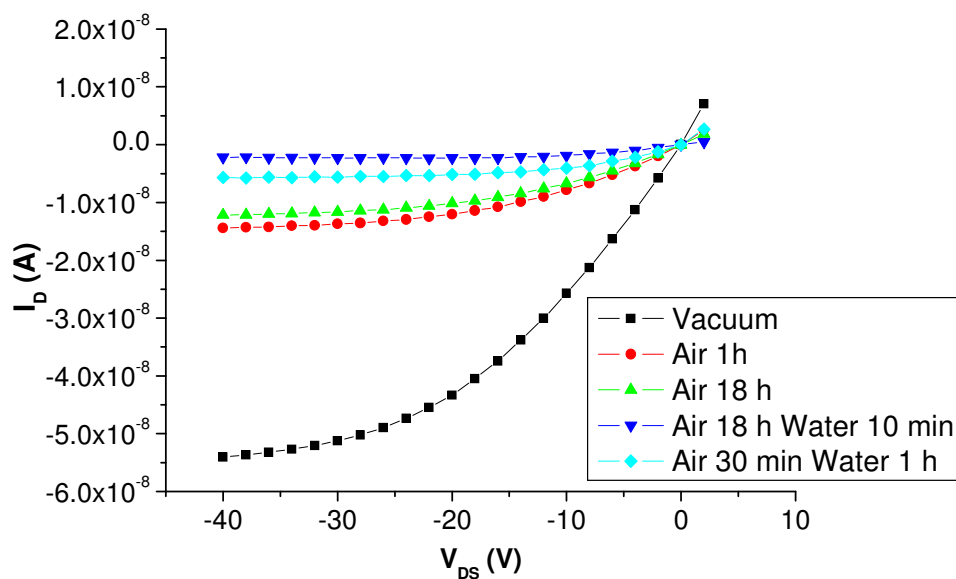


Fig. 23: Comparison of the I/V -characteristics of a FET with unannealed PFTPDA as active layer shown already in figures 15 and 17-20. Here only the curves for $V_{GS} = -40$ V were plotted.

Values for the RR-P3HT in air could not be calculated, since the dependence of the current on the voltage does not obey the conditions set for the validity of equations 4 and 9 so the relations do not hold anymore. In Figure 23 the I/V curves of PFTPDA after exposure to certain conditions are plotted in the same graph for comparison. We can clearly see the influence of air and water on the drain current. The current is lowered by a factor 4 (as is the mobility) in presence of air and the current is lowered by another factor of 2 when water is brought in contact with the sample. This reflects the results for the mobility listed in Table 1.

4 – Conclusions and discussion

The measurements performed on the polymer materials in the FETs in vacuum and in presence of air and water revealed the electrical properties of the two polymers investigated. RR-P3HT is a material which has often been studied and used in organic polymer technology and is used in this research as reference material.

The results shown in paragraph 3.1, the measurements performed in vacuum, which reveal the ‘native’ properties of the materials, give relatively high current and a relatively high mobility, close to $10^{-3} \text{ cm}^2\text{V}^{-1}\text{s}^{-1}$, a value which is in good agreement with the literature values²⁶ for unannealed RR-P3HT. The same measurement performed on a PFTPDA transistor yield a mobility which was a factor 10 lower than the polythiophene mobility and was also quite low compared to mobilities reported for similar polymers (also Polyfluorenediamines) in the literature^{27, 28} which are in the same order of magnitude of the mobilities measured for polythiophenes. These low values combined with the results obtained from the measurements of the HOD and the LED shown in paragraph 3.4, where the current density did not behave accordingly to the space charge limited current model as one would expect, but the current depended on an exponential value of the voltage that was higher than the expected quadratic dependence ($J \sim V^6$), suggesting a trap limited conduction. The conduction through the material seems to be hindered by the presence of multiple traps as it is explained in paragraph 1.1.4. The PFTPDA used was already purified 3 times after its synthesis, and purifying the material only once or twice resulted into very low conduction and poor results. PFTPDA that was purified only once did not show any current in the FET and in the HOD and LED the current through the material was less than an order of magnitude higher than the noise. Impurities from the synthesis might be the cause of the traps in the material, as purification seems to improve greatly the performance of the polymer. Further experiments, such as thickness dependence measurements in HOD and LED, should be performed to prove if indeed the performance of the material is greatly inhibited by traps. When additional experiments clearly suggest that impurities limit the performance of these materials, research how to remove the impurities that cause the traps is to be performed.

The influence of oxygen and water has always been a problem for most semiconducting polymers and organic materials, as they are often degraded in air and in humid conditions. RR-P3HT is known as a chemically air-stable polymer. Molecular oxygen will quickly dope the material as seen in the results presented in paragraph 3.2, but returning the material into vacuum (and eventually heating it up) will free the oxygen fully restoring the material. Water has a more lasting effect on RR-P3HT, permanently degrading the material. On the other hand PFTPDA is more stable in air, not only because it is not degraded, similarly like P3HT, but the doping effect caused by oxygen is also very slow. The mobility of the mobile charges in the saturation regime are preserved and the ON/OFF ratio is still very high. The material remains in stable conditions for several hours. The effect of water on PFTPDA is also less dramatic than on RR-P3HT. The polyfluorene remains quite stable even after one hour of exposure to water. Water does lower the mobility of the charges in the material and the ON/OFF ratio in the FET is also lowered but not under a factor 500, which for measurements purposes is still quite good. Water still degrades PFTPDA however so its stability, as expected, does not hold

indefinitely and the degradation caused by water is irreversible. A problem that arises from the influence of water and oxygen on the material is the increase of the switch-on voltage. This means that to switch on the FET higher gate voltages are needed, sometimes as high as -20 V, which is a very unfavorable property, especially if someone wants to work at low gate voltages or wants to build a device which is sensitive to gate voltage changes around the V_{SO} , like a FET sensor.

We can explain the increased stability of PFTFDA, compared to RR-P3HT, with the picture presented in paragraph 1.2.3. Polyfluorenes in general have a HOMO level situated very deep in energy, around -6 eV compared to vacuum. Polyfluorenes in general are air-stable as one might expect. The presence of the tertiary amine groups in PFTFDA increases the energy of the HOMO level towards -5 V, to improve charge injection from gold, yet the HOMO level of PFTFDA, its energetic position is still undetermined, is probably lower than the HOMO level of RR-P3HT, hence it is more difficult to be oxidized and more difficult to dope as well probably as the doping of the material occurs very slowly under air. The location of the HOMO level of PFTFDA explains its stability towards oxygen and also the partial stability towards water. Although PFTFDA is still degraded the redox reaction with water is slow compared with other polymers, meaning that the HOMO level is still not deep enough to resist oxidation by water.

Other experiments and measurements need to be performed on PFTFDA. First it should be researched if the material can be purified further such that the traps are removed and conduction is improved. A high mobility is very important for semiconductors in electronic devices since a high mobility signifies a better operation at low voltages and a better signal-to-noise ratio. Measurements in water in presence of different ionic species should also be performed on PFTFDA. The ultimate goal is to use the polymer material as active layer in a biosensor. It is thus important to know how the material behaves under the influence of inorganic ions and other charged species.

5 – References

1. Shirakawa H, Ito T, Ikeda S – Makromolekulare Chemie-Macromolecular Chemistry and Physics (1978) 179 (6): 1565-1573
2. Organic chemistry: structure and function, 4th ed. – Vollhardt KPC, Schore NE - New York: Freeman (2003), ISBN: 0-7167-4374-4
3. Hoffmann R, Janiak C, Kollmar C – Macromolecules (1991) 24: 3725-3746
4. Semiconductor devices : physics and technology – Sze SM; New York: Wiley (1985), ISBN: 0-471-87424-8
5. Introduction to semiconductor physics – Grahn HT; Singapore: World Scientific (1999) ISBN: 981-023302-7
6. Electronic processes in organic crystals and polymers, 2nd (rev.) ed. – Pope M, Swenberg CE; New York: Oxford University Press (1999), ISBN: 0-19-512963-6
7. Bassler H - Physica Status Solidi B (1993) 175 (15): 15-56
8. Introduction to Solid State Physics, 8th ed. – Kittel C; Hoboken NJ: Wiley (2005), ISBN: 0-471-68057-5
9. Miller A, Abrahams E – (1960) Physical Review 120 (3): 745-755
10. Polarons & Bipolarons – Alexandrov AS, Mott NF; Singapore: World Scientific (1995), ISBN: 981-022298-X
11. Ziemelis KE, Hussain AT, Bradley DDC, Friend RH – Physical Review Letters (1991) 66 (17): 2231-2234
12. Monroe D – Physical Review Letters (1985) 54 (2): 146-149
13. Horowitz G, Delannoy P – Journal of Applied Physics (1991) 70 (1): 469-475
14. Horowitz G, Hajlaoui R, Delannoy P – Journal de Physique III (1995) 5 (4): 355-371
15. Horowitz G – Solid State Phenomena (2001) 80-81: 3-13
16. Arkhipov VI, von Seggern H, Emelianova EV – Applied Physics Letters (2003) 83: 5074-5076
17. Freire JA, Voss G – Journal of Chemical Physics (2005) 122 (12): Art. No. 124705
18. Meijer EJ, Tanase C, van Veenendal E, Huisman BH, PWM Blom, de Leeuw DM, Klapwijk TM – Applied Physics Letters (2002) 80 (20): 3838-3840
19. Tanase C, Blom PWM, de Leeuw DM, et al. Physica Status Solidi A (2004) 201 (6): 1236-1245
20. Vissenberg MCJM, Matter M – Physical Review B (1998) 57 (20): 12964-12967
21. Charge Transport in Disordered Organic Field-Effect Transistors (PhD Thesis) – Meijer RJ (2003), ISBN: 90-6734-306-4

22. Hamadani BH, Natelson D – Applied Physics Letters (2004) 84 (3): 443-445
23. Taylor DM, Gomes HL, Underhill AE, Edge S, Clemenson PI - Journal of Physics. D (1991) 24: 2032-2038.
24. De Leeuw DM, Simenon MMJ, Brown AR, Einerhand REF – Synthetic Metals (1997) 87: 53-59
25. Electrical Transport in Solids – Kao KC, Hwang W; Oxford: Pergamon Press (1981) ISBN: 0080239730
26. Nguyen PT, Rammelt U, Plieth W – Electrochimica Acta 50 (7-8): 1757-1763
27. Redecker M, Bradley DDC, Inbasekaran M, Wu WW, Woo EP – Advanced Materials (1999) 11 (3): 241-245
28. Campbell AJ, DDC. Bradley – Journal of Applied Physics (2001) 89 (6): 3343-3351